Small RNA Mcr11 regulates genes involved in the central metabolism of *Mycobacterium tuberculosis* and requires 3' sequence along with the transcription factor AbmR for stable expression

Roxie C. Girardin[1] and Kathleen A. McDonough[1,2]*

[1]Department of Biomedical Sciences, School of Public Health, University at Albany, PO Box 22002, Albany, NY 12201-2002

[2]Wadsworth Center, New York State Department of Health

*To whom correspondence should be sent:

Kathleen A. McDonough, PhD

Wadsworth Center

120 New Scotland Avenue

PO Box 22002, Albany, NY 12201-2002

Phone: (518) 486-4253

Fax: (518) 402-4773

Email: kathleen.mcdonough@health.ny.gov

Running Title: Expression and function of mycobacterial small RNA Mcr11

Keywords: sRNA targets, RNA termination, RNA stability, gene regulation, lipoylation

Abstract

Mycobacterium tuberculosis (Mtb), the etiologic agent of tuberculosis, must adapt to host-associated environments during infection by modulating gene expression. Small regulatory RNAs (sRNAs) are key regulators of bacterial gene expression, but their roles in Mtb are not well understood. Here, we address the expression and function of the Mtb sRNA Mcr11, which is associated with slow bacterial growth and latent infections in mice. We found, by using biochemical and genetic approaches, that the AbmR transcription factor and an extended region of native sequence 3' to the *mcr11* gene enhance production of mature Mcr11. Additionally, we found that expression of Mcr11 was unstable in the saprophyte *Mycobacterium smegmatis*, which lacks an *mcr11* orthologue. Bioinformatic analyses used to predict regulatory targets of Mcr11 identified 9-11 nucleotide regions immediately upstream of Rv3282 and *lipB* with potential for direct base-pairing with Mcr11. *mcr11*-dependent regulation of Rv3282, *lipB,* Rv2216 and *pknA* was demonstrated using qRT-PCR in wild type versus *mcr11*-deleted Mtb and found to be responsive to the presence of fatty acids. These studies establish that Mcr11 has roles in regulating growth and central metabolism in Mtb that warrant further investigation. In addition, our finding that multiple factors are required for production of stable, mature Mcr11 emphasizes the need to study mechanisms of sRNA expression and stability in TB complex mycobacteria to understand their roles in TB pathogenesis.

Author Summary

Bacterial pathogens must continuously modulate their gene expression in response to changing conditions to successfully infect and survive within their hosts. Transcription factors are well known regulators of gene expression, but there is growing recognition that small RNAs (sRNAs) also have critically important roles in bacterial gene regulation. Many sRNAs have been identified in *M. tuberculosis* (Mtb), but little is known about their expression, regulatory targets or roles in Mtb biology. In this study, we found that the Mtb sRNA Mcr11, which is expressed at high levels in slowly replicating Mtb and during mouse infection, regulates expression of several target genes involved in central metabolism. Importantly, we also discovered that *mcr11* has unexpected requirements for stable expression in mycobacteria. In particular, we identified RNA sequence elements immediately downstream of *mcr11* that enhance transcription termination and production of mature Mcr11 RNA in TB-complex mycobacteria. Meanwhile, ectopic expression of Mcr11 was unstable in a non-pathogenic strain of mycobacteria, suggesting that factors specific to pathogenic mycobacteria are required for the stable production of Mcr11. These studies identify sRNA stability as a new frontier for understanding gene expression in Mtb.

Introduction

Tuberculosis (TB) remains a major threat to global public health, with at least 10 million new, incident cases and 1.3 million deaths due to TB in 2017 (1). The basic biology of *Mycobacterium tuberculosis* (Mtb), the etiological agent of TB, is poorly understood despite its importance to the development of new therapeutic interventions. Mtb can adopt a specialized physiological state within host tissues, which renders the bacteria phenotypically drug resistant and viable despite extended periods of slow or non-replicating persistence (NRP) (2). NRP and phenotypic drug resistance pose particular challenges for intervention, making it critical to understand the regulatory processes that enable Mtb to adapt to host conditions.

Bacterial and host factors that contribute to NRP and slow growth are still being defined (3). Host-associated environmental cues that result in metabolic remodeling and a shift away from active growth toward a state of persistence include hypoxia, nitrosative stress, redox stress, nutrient starvation, as well as adaptation to cholesterol and fatty acid metabolism (4-9). Isocitrate lysases (ICLs) are used by bacteria to maintain growth on fatty acids through the glyoxylate shunt, and are critical for Mtb's ability to survive on fatty acids and within the host (10-12). Surprisingly, ICLs are also required for growth on carbohydrate carbon sources (13), and gluconeogenesis is required for Mtb virulence (14-16). Additionally, lipoylated enzymes involved in the citric acid cycle, such as lipoamide dehydrogenase (Lpd) and dihydrolipoamide acyltransferase (DlaT), are necessary for Mtb survival in the host and viability

during NRP (17-19). However, factors that regulate these processes are not well understood.

Gene expression studies have provided critical insights into the regulation and function of proteins like transcription factors that modulate gene expression as Mtb adapts to the host environment during infection (20, 21). The additional role of sRNAs in gene regulation is recognized in other bacteria (22), and several sRNAs whose expression is responsive to stress and/ or growth phase have been identified in mycobacteria (23-28). (23-26, 29-31). It also has been observed that over expression of some sRNAs leads to slow or delayed growth in mycobacteria (23, 32). However, the importance of these differentially expressed sRNAs to the adaptation and survival of Mtb during periods of stress has not been fully addressed.

The intergenic sRNA Mcr11 (*ncRv11264Ac*) is one of the best-studied mycboacterial sRNAs (24, 26, 29, 33). Expression of Mcr11 is regulated in response to advanced growth phase and levels of the universal second messenger 3',5'-cyclic adenosine monophosphate (cAMP) (24, 26, 29). Additionally, Mcr11 is abundantly expressed by Mtb in the lungs of chronically infected mice (26) as well as in hypoxic and non-replicating Mtb (32). Transcriptional regulators of *mcr11* expression include the product of the adjacent, divergently expressed gene *abmR* (*Rv1265)* (33), and the cAMP binding transcription factor (TF) CRP_{MT} (29). The structure and function of Mcr11 in TB-complex mycobacteria is unknown, prompting us to further characterize this sRNA.

Here, we report that cis-acting, extended, native sequence 3' to Mcr11 enhances production of Mcr11 in mycobacteria. Optimal Mcr11 termination efficiency needed the transcription factor AbmR and was regulated by growth phase in Mtb and *Mycobacterium bovis* BCG, but not in the fast-growing saprophyte *Mycobacterium smegmatis*. We found that *mcr11* regulates expression of *lipB* and *Rv3282,* which contribute to central metabolic pathways associated with NRP and slow growth in Mtb. In addition, Mcr11 affected growth of both Mtb and BCG in hypoxic conditions without fatty acids. This study identifies TB complex-specific cis and trans factors required for stable Mcr11 expression while providing the first report of *mcr11*-dependent regulation of gene targets in Mtb.

Results

Modeling secondary structure of Mcr11

Previous studies established two 5' ends of Mcr11 at chromosomal positions 1413224 and 1413227 in *Mycobacterium tuberculosis* H37Rv (24, 29), but the 3' end of Mcr11 is poorly defined. Preliminary efforts to express Mcr11 based on size estimates from prior Northern blot experiments were not successful, despite the well-mapped 5' end of the sRNA. Secondary structural features of sRNAs greatly contribute to their function, and RNA folding is most strongly influenced by the nucleotide sequence of the RNA (34, 35). We reasoned that defining the precise boundaries of Mcr11 could help in identifying its function.

We mapped the 3' end of Mcr11 to chromosomal positions 1413107 and 1413108 in *Mycobacterium tuberculosis* (Mtb) using 3' rapid amplification of cNDA ends (RACE) and Sanger sequencing (Figure 1A). These 3' ends are 120 and 119 nucleotides (nt) downstream from the most abundant previously mapped 5' end at position 1413227 (24). Our mapped 3' ends vary 3-4 nucleotides from the 3' end at chromosomal position 1413111 inferred by deep sequencing (36), and are 13-14 nt shorter than the 3' end estimated by cloning (24) (Figure 1A). These results indicate that Mcr11 is a transcript between 117 and 121 nt long, which is consistent with its observed size by Northern blot (24, 26, 29).

The mapped 3' ends of Mcr11 at chromosomal positions 1413107/ 1413108 varied by 3-13 nt from previous estimates of the 3' end of Mcr11, so we considered the possibility that this variance could be functionally significant.

Transcriptional termination occurs in prokaryotes by two described mechanisms: Rho-dependent termination and intrinsic, Rho-independent termination (37-39). Rho-dependent termination requires the association of the ATP-hydrolyzing molecular motor Rho with the nascent RNA, which is typically cytosine-enriched, guanosine-depleted and unstructured at the 3' end (40). Intrinsic, Rho-independent termination is governed by the formation of a structured termination hairpin that is usually followed a poly-U tail, and is highly dependent upon the sequence of the nascent RNA. Several mycobacterial sRNAs have multiple reported 3' ends, suggestive of Rho-dependent termination and/or post-transcriptional processing (23, 30, 31). However, relatively little is known about transcriptional termination in Mtb, particularly at sRNAs (41-45).

We modeled the secondary structure of Mcr11 with varying lengths of extended, native 3' RNA sequence by using RNA Structure (46) to reveal potential functional features. Mcr11 was predicted to be highly structured, with few single-stranded (ss) regions available for potential base-pairing with regulatory target RNA sequences (Figure 1B). Use of either mapped 5' end of *mcr11* produced the same Mcr11 secondary structure, as these 5' nucleotides are predicted to be unpaired (Figure 1B). Modeled structures of extended native sequence 3' to our mapped ends of *mcr11* revealed additional highly structured motifs with similarity to predicted Rho-independent terminators (RITs) downstream of *mcr11* in mycobacteria (43, 44). However, none included the long, characteristic poly-U tail found in RITs of other bacteria (38). A 10 nt region containing a sub-optimal poly-U tract was identified by scanning sequence

173 downstream of the mapped 3' end of Mcr11 in the constructs that contained 3'
174 sequence elements (TSEs) 2-4 (Figure 1A). Modeling the secondary structure of
175 this sequence revealed a stem loop structure with a 7nt trail containing 4
176 discontinuous Us (Figure 1C).
177
178 ***Measurement of TSE function in Msm***
179 We tested the impact of different *mcr11* TSEs on the transcriptional
180 termination of Mcr11 using promoter:*mcr11:TSE:GFPv* reporter constructs
181 (Figure 2A-B). We reasoned that transcriptional termination levels could be
182 inferred by using GFPv fluorescence as a relative measure of transcriptional
183 read-through beyond the *mcr11* gene (Figure 2A). The relative percentage of
184 termination for each TSE was calculated by dividing the observed fluorescence
185 of each P*mcr11:TSE:GFPv* strain by the observed fluorescence of an *mcr11*
186 promoter-only:*GFPv* construct (P*mcr11:GFPv*), subtracting the product from 1,
187 and multiplying the result by 100. Promoterless *GFPv* served as a negative
188 assay control, and an *mcr11*-independent promoter:*GFPv* fusion construct
189 served as a positive assay control. A positive intrinsic termination control was
190 generated by fusing *mcr11* and a small amount of native 3' trailing sequence to a
191 synthetic RIT ($tt_{sbi}B$) that has been shown to function at ~98% efficiency with Mtb
192 RNAP *in vitro* (Figure 1B) (42).
193 Our initial termination experiments measuring TSE efficiency were
194 performed in Msm, because it lacks an *mcr11* orthologue and thus has no basal
195 Mcr11 expression. The inclusion of any TSE sequence at the 3' end of *mcr11*

196 resulted in decreased transcriptional read-through of the *mcr11*:GFPv fusion
197 reporter, as compared to the relative levels of GFPv fluorescence for P*mcr11*
198 alone (Figure 2B). This result suggested that all TSEs supported transcriptional
199 termination to varying degrees. Longer TSEs had greater termination efficiency,
200 but the positive $tt_{sbi}B$ intrinsic termination control exhibited the strongest mean
201 termination efficiency at 88% (Figure 2C). Paraformaldehyde-fixed duplicates of
202 each sample were subjected to flow cytometry analysis to determine if the mean
203 GFPv fluorescence observed in our plate-based assay was reflective of the
204 fluorescence observed in individual cells, or if there were populations of cells with
205 varying levels of fluorescence. A single, homogenous population of fluorescent
206 cells was observed for each reporter, demonstrating that mean fluorescence
207 measured in the plate reader assay was representative of the fluorescence in
208 individual cells (Supplemental Figure 2). From these data, we concluded that
209 mean fluorescence reflected relative termination efficiency for each TSE reporter.
210 Northern blot analysis was performed to further evaluate the expression of
211 Mcr11 in Msm. We noted that the size of Mcr11 did not vary in Msm despite the
212 presence of TSEs with various lengths, suggesting that TSEs are rapidly
213 processed off of the mature sRNA if they are transcribed (Figure 2D). Mcr11 was
214 also present at very low levels in Msm when compared to a BCG control for
215 which 1/3 the amount of total RNA present in the Msm samples was loaded in
216 the gel (Figure 2D). These results are consistent with the possibility of reduced
217 Mcr11 expression and/or stability in Msm compared to BCG.
218

TB complex- specific factors are required for stable Mcr11 expression

mcr11 expression varies across growth phases in TB complex mycobacteria (24, 33), so we examined the effect of growth phase on *mcr11* expression in Msm. Fluorescence from the GFPv transcriptional reporters was measured at mid-log and late stationary phase. Surprisingly, we observed that P*mcr11* activity was not increased by advancing growth phase when expressed in Msm (Figure 2E), suggesting that a positive regulatory factor was absent.

Previously, we showed that the divergently expressed DNA-binding protein AbmR is a growth phase-responsive activator of *mcr11* expression (33). Although the Msm orthologue (*MSMEG_5010)* of *abmR* displays both high amino acid sequence identity (68.75%) and amino acid similarity (83.51%) to AbmR (33), we hypothesized that *abmR* has functionality that the Msm orthologue lacks. Thus, we added a copy of the Mtb *abmR* locus upstream of the P*mcr11*::*GFPv* fusion sequences and tested the activity of P*mcr11* in response to growth phase in Msm. The addition of *abmR* significantly increased P*mcr11* activity in Msm, and rendered P*mcr11* activity responsive to growth phase (Figure 2E), as previously observed in BCG and Mtb (33). However, inclusion of *abmR* did not significantly increase the amount of stable Mcr11 detected by Northern blot in Msm (Figure 2D), indicating that Mcr11 is unstable when transcribed in Msm. Together, these results show that Mtb *abmR* regulates *mcr11* expression at the transcriptional level, but is not sufficient for stable Mcr11 expression in a non-native environment.

Further studies in TB-complex mycobacteria showed that the termination efficiencies of *mcr11* TSEs in mid-log phase BCG were similar to those observed in Msm (Figure 3), but only BCG showed enhanced *mcr11* TSE termination efficiencies in late stationary phase. This growth-phase dependent increase in termination efficiency in BCG was strongest for TSE1, which improved from approximately 40% to 70% (Figure 3C). Overall termination efficiencies of *mcr11* TSEs were also greater in virulent Mtb (H37Rv) than in BCG or Msm (Figure 3D-F). Deletion of *abmR* caused a small but significant decrease in *mcr11* termination efficiencies from all constructs, with the TSE1 short hairpin being the most strongly affected (Supplemental Figure 3). Together, these data indicate that multiple trans-acting factors specific to the genetic background of TB-complex mycobacteria facilitate the transcriptional termination and production of stable Mcr11.

Longer TSEs enhance expression of Mcr11 in TB-complex mycobacteria

We expected that increased termination efficiencies would correlate with higher levels of mature Mcr11 in TB complex mycobacteria. Thus, we used Northern blot analyses to measure the production of stable Mcr11 from various *mcr11* TSE constructs in *Δmcr11* strains of BCG and Mtb during late stationary phase (Figure 4). Robust levels of Mcr11 were produced from constructs containing native *mcr11* TSEs. As was observed in experiments with Msm, Mcr11 size remained constant despite its expression with TSEs of different

lengths in BCG or Mtb (Figure 4). This size restriction is consistent with precise termination or an RNA processing event that produces discrete 3' ends.

We considered the possibility that expression of *mcr11* in the context of an mRNA with a translated, stable transgene such as *GFPv* could contribute to the stability of Mcr11. Production of Mcr11 from *mcr11*:TSE1 constructs was compared to Mcr11 levels from a similar construct in which *GPFv* is not immediately downstream of TSE1 (Figure 5A). Mcr11 levels were not affected by the GFPv location (Figure 5B), indicating that *GFPv* did not contribute to the production or processing of stable Mcr11 in these experiments. This conclusion is also consistent with the low levels of Mcr11 observed in Msm despite the presence of the *GFPv* transgene (Figure 2D).

As advancing growth phase significantly improved the termination efficiencies of TSEs in BCG (Figure 3C), we tested the effects of growth phase on the expression of *mcr11*. Mcr11 levels were observed by Northern blot (Figure 5C) and measured by qRT-PCR (Figure 5D) in BCG*Δmcr11* strains carrying ectopic copies of either *mcr11*:TSE1 or *mcr11*:TSE3. Both constructs showed growth-phase dependent increases in expression of stable Mcr11 (Figure 5C and 5D). Stress conditions can modulate the efficiency of RITs (47) and induce the appearance of multiple, different size products of a single sRNA in Mtb (23, 27). However, neither BCG nor Mtb displayed significant stress-induced changes in the termination efficiencies of *mcr11* TSEs (Supplemental Table 3) when subjected to nitrosative stress (DETA-NO), ATP depletion (BDQ), DNA damage

(OFX), or transcriptional stress (RIF). These data demonstrate the significant role that differences in native 3' sequence have on stable Mcr11 expression.

Identification of Mcr11 regulatory targets

Having identified the sequence features required for robust ectopic production of Mcr11 in complemented *Δmcr11* strains, we considered *mcr11* function. A bioinformatic search of potential regulatory targets of Mcr11 using TargetRNA (48) and TargetRNA2 (49) identified *abmR* as the top-scoring hit (Figure 6A) (Supplemental Table 4). We measured the relative abundance of AbmR protein by Western blot analysis, and found that it was decreased in BGC*Δmcr11* and Mtb*Δmcr11* (Figure 6B,C). However, recent reports indicate that the *abmR* mRNA is a leaderless transcript that lacks a 5' UTR (50), so the region of direct base-pair complementarity with the Mcr11 sRNA and the 5' end of *abmR* predicted by TargetRNA is not likely to be present in the *abmR* mRNA (50). We also previously showed that the *mcr11* gene overlaps a substantial portion of the DNA sequences identified as the upstream enhancer and promoter regions for *abmR* transcription (Figure 6A) (33, 51).

We addressed the possibility that *mcr11* deletion has cis rather than trans effects on *abmR* expression due to disruption of *abmR* regulatory sequences. Promoter:*lacZ* reporter studies were used to compare P*abmR* activity in the presence and absence of flanking *mcr11* sequences in Wt BCG and Mtb backgrounds that express Wt levels of Mcr11. Transcriptional activity from the minimal *abmR* promoter lacking adjacent sequence in the *mcr11* gene was much

lower than that from the extended *abmR* promoter that includes contiguous *mcr11* gene sequences (Figure 6D). These assays were conducted in the Wt backgrounds of BCG and Mtb with comparable levels of native *mcr11* expression in all matched strains, indicating that sequence overlapping the *mcr11* gene was required in cis for full *abmR* promoter activity. We conclude that the reduced expression of *abmR* in *Δmcr11* strains is likely due to the loss of sequence-based *abmR* regulatory elements within the *mcr11* gene rather than a trans-acting regulatory effect of Mcr11 on *abmR* expression.

TargetRNA also predicted multiple putative targets of Mcr11 regulation, including two genes within operons involved in central metabolic processes and cell division: *lipB* (encodes lipoate protein ligase B, needed for lipoate biosynthesis) (Figure 7A) and *Rv3282* (encodes a conserved hypothetical protein with homology to Maf septum-site inhibition protein) (Figure 7B). The intergenic spacing between putative target gene *fadA3* (*Rv1074c)*, which encodes a beta-ketoacyl coenzyme A thiolase, and the preceding gene (*Rv1075c*) is identical to that of the intergenic spacing between *Rv2216* and *lipB*. However, *fadA3* is likely to be transcribed independently of *Rv1075c* (50). *lipB* and Rv3282 were selected for follow-up because they are essential, associated with growth and central metabolism of Mtb, and contain predicted Mcr11 base-pairing sequences that are within known mRNA transcript boundaries. Each of these target transcripts has the potential to interact with Mcr11 through a 9-11 nt continuous base pairing region, followed by a shorter stretch of gapped or imperfect base pairing (Figure 7A and 7B). A region from nt 39-55 of Mcr11 was predicted to interact with these

mRNA targets and others (Figure 7C and 7D, Supplemental Table 4), which includes a region of Mcr11 predicted to be in an unpaired loop in multiple modeled secondary structures of Mcr11 (Supplemental Figure 4).

Fatty acids affect Mcr11-dependent regulation of target genes in Mtb

The *lipB* operon includes *dlaT*, which encodes DlaT, the E2 component of pyruvate dehydrogenase (PDH) and the peroxynitrite reductase/peroxidase (PNR/P) complex in Mtb. The function of DlaT is modulated by lipoylation, which is dependent upon lipoate biosynthesis by LipB (18, 52). BkdC (also called PdhC or Rv2495c) is a component of the branched chain keto-acid dehydrogenase (BCKADH) complex in Mtb that also requires lipoylation for activity. Disruption of components in any of these complexes can cause growth defects in Mtb, some of which are dependent upon the nutrient mixture present in the growth media (18, 19). The genes upstream of Rv3282 are *accD5* and *accE5*, which are needed for a long chain aceyl-CoA carboxylase enzymatic complex that generates substrates for fatty acid and mycolic acid biosynthesis (53, 54).

We used qRT-PCR to measure expression of genes within the operons containing predicted Mcr11-regulatory targets *lipB* and Rv3282 in Wt versus *⊿mcr11* strains. Gene expression was queried in stationary phase BCG and Mtb grown in media with (+OA) or without (-OA) fatty acids to assess the impact of Mcr11 regulatory function in these conditions. Tween-80® is a hydrolysable detergent that can release a substantial amount of fatty acids (primarily oleic acid), and so was replaced with the non-hydrolysable detergent Tyloxapol in media lacking fatty acids. The *mcr11* complements included TSE4 with or without

355 an intact copy of *abmR*. Levels of *phoP*, a response regulator expected to be
356 independent of *mcr11* and *abmR*, and *pknA*, a serine-threonine protein kinase
357 required for growth, were also measured.

358 Expression of *Rv3282*, Rv2216, *lipB* and *pknA* was significantly de-
359 repressed in Mtb*Δmcr11* compared to Wt Mtb in the absence, but not the
360 presence, of fatty acids. In contrast, levels of *lipB* and *pknA* expression
361 decreased in the *mcr11* Mtb mutant when fatty acids were present.
362 Complementation of *mcr11* fully (Rv3282, *pknA*) or partially (Rv2216, *lipB*)
363 restored expression to Wt levels (Figure 8A). The expression of *accD5* (Rv3280)
364 was significantly de-repressed and *accE5* (Rv3281) trended toward de-
365 repression in Mtb*Δmcr11*, and complementation partially restored Wt levels of
366 expression of both genes (Supplemental Figure 5A). Expression of *dlaT* and
367 *phoP* were not altered in Mtb (Figure 8A). From these data, we concluded that
368 Mcr11-mediated regulation expression of *Rv3282*, *Rv2216*, *lipB* and *pknA*
369 expression in stationary phase Mtb is affected by the levels of fatty acids in the
370 media. In contrast, no Mcr11-dependent regulation of the putative target genes
371 was observed in BCG other than a trend of higher *Rv3282* expression in
372 BCG*Δmcr11* relative to Wt BCG (Figure 8C and 8D). These data demonstrate
373 that *mcr11*-dependent regulation of specific target genes is responsive to the
374 fatty acid content of the culture media, and suggest that Mcr11 has a role in
375 regulating the central metabolism of Mtb.

376 Expression levels of mRNA do not always match expression levels of the
377 cognate protein if a gene is subjected to multiple layers of regulation. We tested if

the protein levels of PknA or lipoylated DlaT were altered in Mtb*Δmcr11* by Western blot. No significant differences in the abundance of PknA or lipoylated DlaT were observed between Mtb*Δmcr11* and Wt Mtb (Supplemental Figure 5B). It is possible that de-repression of *lipB* does not affect DlaT lipoylation if lipoate is limiting or if wild-type levels are already saturating for lipoylation of DlaT.

Mcr11 is required for optimal growth of BCG and Mtb without fatty acids

Optimal growth of Mtb on carbohydrate-based carbon sources requires appropriate *dlaT* expression (18, 19) and *lipB, accD5,* and *accE5* are essential for the growth of Mtb (55, 56). Mutations in *Rv3282* delay Mtb growth, even in nutrient rich media (55). Based on our observed regulation of these genes by Mcr11, we hypothesized that *Δmcr11* deleted strains would exhibit a growth defect when forced to utilize carbohydrate carbon sources for growth in media lacking a source of fatty acids.

No growth differences were observed between Wt and *Δmcr11* mutant Mtb or BCG in media containing fatty acids. However, BCG*Δmcr11* was severely growth-lagged and Mtb*Δmcr11* was moderately growth delayed compared to Wt bacteria when grown in media lacking fatty acids (Figure 8E-H). Complementation with *mcr11* partially complemented growth in BCG and fully restored growth to Wt levels in Mtb (Figure 8G and 8E). From these data, we conclude that *mcr11* has a role in the central metabolism and growth of BCG and Mtb.

Discussion

This work identifies several genes associated with central metabolism in Mtb as regulatory targets of the sRNA Mcr11. We also demonstrated that transcriptional termination and stable production of the sRNA Mcr11 is enhanced by extended native sequence 3' to *mcr11* along with the product of the divergently transcribed adjacent gene, *abmR*. The regulation of central metabolism in Mtb is consistent with *mcr11* expression profiles in response to growth phase and *in vivo* infection (26, 33). However, the additional requirements for TB complex specific factors for stable Mcr11 expression were unexpected, and this may have broader implications for understanding sRNA expression in Mtb.

Characterization of the factors required for efficient termination and stable expression of Mcr11 was a prerequisite for the complementation studies that confirmed Mcr11 regulatory targets. Protein coding mRNAs often can tolerate variable amounts of 5' and 3' flanking sequence because the signals for protein expression are provided immediately upstream and within the open reading frame (ORF). In contrast, expression of functional sRNAs may be more dependent on RNA chaperones and/or processing factors, as well as cis-acting sequence elements at their transcriptional boundaries that may be difficult to define (25, 47, 57-59). Defining the role of these cis-acting sequences for *mcr11* and possibly other sRNAs in Mtb is an important topic for future studies.

Mechanism of mcr11 transcriptional termination

Sequences at the 3' end of sRNAs can be critical for stability, function and interaction with RNA chaperones, although such chaperones have yet to be identified in mycobacteria (25, 59-64). The role of extended native 3' sequences for expression of mycobacterial sRNAs warrants further investigation to determine whether *mcr11* is exceptional or representative of a larger group of sRNAs with regards to expression and stability requirements.

A recent study of Rho function in Mtb (41) found that depletion of Rho did not impact transcriptional boundaries at predicted RITs (43, 44), demonstrating a clear separation in the populations of transcripts terminated by RITs and Rho-dependent mechanisms. While we found that TSEs promote expression of Mcr11, their underlying mechanism remains unclear and our data do not precisely fit either the current RIT or Rho-dependent termination models (Table 1). We propose a model in which *mcr11* processing occurs immediately following, or concurrent with, Rho-dependent termination.

Table 1: Comparison of transcription termination types

Features	Rho-Dependent	Intrinsic	Mcr11
Predicted hairpin in 3' sequence		✔	✔
Unstructured, C-rich 3' sequence	✔		
Poly U-tract in 3' sequence		✔	
Extrinsic factor(s) required	✔		✔
Transcription factor may impact functionality	✔	✔	✔

443 Rho-independent termination is considered “intrinsic” because extrinsic
444 accessory factors are not required for function (38). Our results clearly indicate
445 that production of stable Mcr11 requires factors other than the TSEs (Figs. 2D
446 and 4). The species-specific effects we observed for *mcr11* termination
447 measured by the GFPv reporter assays suggest that bacterial-specific factors
448 affect the efficiency of *mcr11* termination itself, although the effects on Mcr11
449 stability are more striking (Figs. 2-4).

450 Rho utilization (rut) sites are degenerate and difficult to predict using
451 bioinformatics approaches, but transcripts terminated by Rho tend to have C-
452 enriched, G-depleted 3’ ends that are thought to be unstructured (40). It is not
453 clear if there is a rut site within *mcr11*, as the sequences downstream of the 3’
454 end of Mcr11 are predicted to be highly structured and are rich in both G and C
455 (Fig. 1). A run of 6Cs (nucleotides 93-98) occurs within Mcr11, but this region
456 may be highly structured (Fig. 1). In contrast, Mcr11 TSEs 2-4, which contributed
457 strongly to the termination of Mcr11, all possess C-rich loops in their predicted
458 secondary structures that could be rut sites (Fig. 1). Rho-significant regions
459 (RSRs) reported in the Botella et al study (41) include an RSR that begins 6 nt
460 downstream of the mapped 3’ end of Mcr11, that is characterized as a region of
461 general antisense transcription. The presence of this RSR is consistent with the
462 possibility that *mcr11* expression is Rho-terminated. Mcr10 (*ncRv1157a*) is also
463 proximal to an RSR (41). Future work is needed to establish the importance of
464 Rho-dependent termination for mycobacterial sRNAs.

In *Escherichia coli*, multiple trans-acting factors are known to modulate termination and anti-termination of Rho-terminated sRNAs (65). AbmR, an ATP-responsive DNA-binding transcription factor that activates *mcr11* expression (33), was found here to also positively regulate termination efficiency of *mcr11*. Despite the high similarity between *abmR* and its Msm orthologue (33), *MSM_5010* failed to strongly activate *mcr11* expression and Mcr11 transcripts were unstable in Msm, even when *abmR* was provided in trans. It is possible that AbmR interacts directly with RNAP or Rho to affect termination, or recruits an as yet undefined trans-acting factor that modulates Mcr11 termination in Mtb. It will also be important to determine which specific sequence or structural elements in the TSEs of *mcr11* contribute to transcriptional termination versus processing, and the extent to which similar TSEs are associated with other sRNAs in mycobacteria.

The discrete 3' end of mature Mcr11 observed by Northern blot is consistent with a processed or precisely terminated RNA, as transcription through TSEs would otherwise result in RNAs significantly longer products. Processing of the 3' ends of mycobacterial sRNAs has been proposed (31), and a recent report identified a hypoxia-regulated mycobacterial sRNA that is extensively processed at its 3' end (25). The observed size variants of specific sRNA species in response to host-associated stress conditions (23) provide further evidence for processing of sRNAs in mycobacteria.

Processing mechanisms for tRNAs and sRNAs have been defined, particularly for transcripts terminated by RITs in *E. coli* (57, 66-70). Recent work

488 has demonstrated that Rho terminated transcripts have processed 3' ends
489 immediately downstream of a stable stem-loop (71). The processing of these
490 discrete ends is dependent on the redundant action of the 3' → 5' exonucleases
491 PNPase and RNase II, and it was speculated that the stem-loop promotes
492 stabilization of the processed transcript (71). While few RNA processing
493 enzymes of mycobacteria have been well characterized, the Mtb genome
494 encodes many known RNases with varying sequence specificities (72-77). We
495 speculate that unidentified TB-complex RNA chaperones and/or modifying
496 enzymes contribute to Mcr11 stability, and that their absence in Msm results in
497 Mcr11 degradation.
498
499 ***Regulation of predicted targets of Mcr11***
500 Oleic acid is the main fatty acid present in rich mycobacterial media
501 formulations, provided either directly as oleic acid or in the hydrolyzable, nonionic
502 detergent Tween-80®. The presence of Tween-80® can alter acid resistance
503 (78), enhances the growth of mycobacteria when combined with glucose or
504 glycerol (79, 80), and increases the uptake of glucose by BCG (79, 80). While we
505 did not observe sensitivity to acid in BCG*Δmcr11* or BCG*ΔabmR* (data not
506 shown), *mcr11* was required for growth on media lacking added fatty acids.
507 Nutrient rich media is often used in batch culture experimentation with Mtb, and
508 the potential confounding effect of multiple nutrient sources on characterizing the
509 essentiality and function of gene products has recently gained appreciation (36,
510 81). Future studies characterizing nutrient uptake in Mtb and BCG strains of

511 *Δmcr11* or *ΔabmR* will further our understanding of the nutrient related growth
512 defects of these strains.

513 Two metabolic enzymes critical for Mtb pathogenesis are known to be
514 lipoylated in Mtb, including dihydrolipoamide acyltransferase (DlaT) and BkdC, a
515 component of the Lpd-dependent branched chain keto-acid dehydrogenase
516 (BCKADH) (18). Lipoylation in Mtb is presumed to depend solely on lipoate
517 synthesis by the enzymes LipA and the Mcr11 target LipB, as scavenging and
518 import pathways are apparently lacking (52). *Rv3282* has homology to Maf, a
519 septum inhibition protein conserved across all domains of life (82, 83). It is in a
520 putative operon with *accD5* and *accE5*, which encode a probable propionyl-
521 coenzyme A carboxylase involved in the detoxification of propionate using the
522 methylmalonyl pathway to produce methyl-branched virulence lipids (84). Despite
523 *mcr11*-dependent regulation of *Rv3282* in the absence of fatty acids, Mtb*Δmcr11*
524 did not have a filamentous cell morphology (data not shown) and the function of
525 Rv3282 in Mtb has not been defined. The regulation of Mcr11's targets was
526 responsive to the fatty acid content of the growth media, and it will be important
527 to determine if the observed growth defects of Mtb*Δmcr11* are due to the
528 dysregulation of *lipB* and *Rv3282*, or if there are additional targets of Mcr11
529 regulation that account for this phenotype (Figure 9). Additionally, the role of
530 Mcr11 in supporting the growth and persistence of Mtb in response to nutrient
531 availability and growth arrest should be explored.

532 Mcr11-dependent regulation of *lipB* and *Rv3282* expression is expected to
533 occur through base-paring with the mRNA, although future work is needed to

534 establish the mechanism (Figure 7). The sRNA RyhB is known to differentially
535 regulate expression of individual genes within the *iscRSUA* operon, resulting in
536 down-regulation of the *icsSUA* genes while maintaining expression of *iscR* (85).
537 This mechanism requires an intra-cistronic base-pairing dependent translational
538 blockade of *iscS*, followed by recruitment of RNaseE and selective degradation
539 of the 3' end of the mRNA. The position of both putative Mcr11 base-pairing sites
540 within target gene operons raises multiple possibilities for *mcr11*-mediated
541 regulation of co-transcribed genes that will be an intriguing topic for future study.
542 We noted that the *mcr11* target interaction site within the intergenic region of
543 *Rv2216* and *lipB* had identical spacing to that of *Rv1075c* and *fadA3*, although
544 the significance of this architecture is unknown.

545 This study shows that the transcriptional termination and stability of the
546 sRNA Mcr11 is enhanced by extended, native 3' sequence elements (TSEs) in
547 TB complex mycobacteria. The role of AbmR in *mcr11* expression was extended
548 from that of a transcriptional activator to include enhancement of *mcr11*
549 transcriptional termination. Our observation that bacterial-species specific factors
550 govern sRNA stability in mycobacteria may also extend to other sRNAs.
551 Combined use of bioinformatic and molecular tools established fatty acid
552 responsive, *mcr11*-dependent gene regulation in Mtb and provides a versatile
553 strategy for the continued search of sRNA function in pathogenic mycobacteria.
554 Future work defining the precise roles of the sRNA Mcr11 in regulating the
555 growth and metabolism of Mtb will greatly advance our understanding of this
556 important pathogen.

Materials and Methods

Bacterial Strains and Growth Conditions

Mycobacterium tuberculosis H37Rv (Mtb) (ATCC 25618) and *Mycobacterium bovis* BCG (BCG) (Pasteur strain, Trudeau Institute) were grown on 7H10 agar (Difco) supplemented with 10% oleic acid-albumin-dextrose-catalase (OADC) (Becton Dickson and Company) and 0.01% cyclohexamide or in Middlebrook 7H9 liquid medium (Difco) supplemented with 10% (vol/vol) OADC, 0.2% (vol/vol) glycerol, and 0.05% (vol/vol) Tween-80 (Sigma-Aldrich) in physiologically relevant shaking, hypoxic conditions (1.3% O_2, 5% CO_2) (86) for promoter::reporter fusion assays and Northern blot analysis. *Mycobacterium smegmatis* mc^2155 (Msm) (ATCC 700048) was grown in Middlebrook 7H9 liquid medium (Difco) supplemented with 10% (vol/vol) OADC, 0.2% (vol/vol) glycerol, and 0.05% (vol/vol) Tween-80 (Sigma-Aldrich), shaking in ambient air for promoter::reporter fusion assays and Northern blot analysis. All experiments were started from low-passage frozen stocks. For cloning experiments, *Escherichia coli* strains were grown on Luria-Bertani (Difco) agar plates or in liquid broth. Growth media and plates were supplemented with 50 μg/mL hygromycin, 25 μg/mL kanamycin (Sigma-Aldrich) for selection of clones. All bacterial cultures were incubated at 37°C.

Mutant Strain Construction

Knockout strains of *mcr11* in Mtb and BCG genetic backgrounds were generated using homologous recombination (87) to replace nucleotides 1-100 with a hygromycin resistance cassette. Disruption of *mcr11* was confirmed with

polymerase chain reaction (PCR) (Supplemental Figure 1B. and 1C.) and Northern blot analysis (Supplemental Figure 1D. and 1E.). Several complementation constructs were created to restore Mcr11 expression. Sequence from the corrected *abmR* (*Rv1265)* start site (51) to the end of the *Rv1264* ORF was amplified by PCR and cloned downstream of the *efTu* (Rv0685) promoter in the multi-copy plasmid pMBC280, creating pMBC1211. PCR was used to amplify varying lengths of sequence from the end of the *Rv1264* ORF through the end of the *abmR* ORF, and they were cloned it into pMBC409, which contains a kanamycin resistance marker, to create pMBC2040, pMBC2041, and pMBC2042 (Supplemental Figure 1A.). Complementation plasmids were sequenced to verify that the desired sequences had been correctly incorporated and then used to transform Mtb and BCG by electroporation. A complete list of plasmids used in this study are provided in Supplemental Table 1 and primers are listed in Supplemental Table 2.

Mapping the 3' End of Mcr11

RNA was harvested from late-log phase Mtb and the 3' end of Mcr11 was mapped using the miScript Reverse Transcription Kit (Qiagen) (88) and a gene-specific primer. The reaction product was cloned into pCRII-TOPO vector (Life Technologies) and ten positive clones were subjected to Sanger sequencing. The sequences were mapped back to the chromosome of Mtb.

Bioinformatic Modeling of Mcr11

Secondary structure modeling of Mcr11 and putative native intrinsic terminators was performed using RNAstructure using default parameters (46).

Color-coded base-pair drawings of predicted RNA secondary structures were created with Visualization Applet for RNA (VARNA) (89) and simplified line drawings were made in Inkscape (inkscape.org). A synthetic terminator ($tt_{sbi}B$) (90) was modeled onto Mcr11 as well. Secondary structure modeling of Mcr11 was performed using RNAstructure (46). Using the previously published 5' and 3' boundaries of Mcr11, minimum free energy (MFE) and centroid structures for Mcr11 derived from CentroidFold (using the CONTRAfold inference engine), Mfold, NUPACK, RNAfold, and RNAStructure algorithims were created (46, 91-94). Base-pair drawings of predicted RNA secondary structures were either directly exported from the software used, or created with Visualization Applet for RNA (VARNA) (89) and simplified line drawings were made in Inkscape (inkscape.org).

Regulatory targets of Mcr11 in Mtb were predicted using TargetRNA (48) and TargetRNA2 algorithms (49), set to default parameters (Table3). Where possible, the position of predicted regions of base-paring between Mcr11 and a putative regulatory target were evaluated against known 5' ends of mRNAs in Mtb (50) (Table 3).

Promoter::Reporter Fusion Assays

Promoter:l*acZ* fusions were created to compare the relative transcriptional activities from DNA sequences spanning the intergenic space between *Rv1264* and *abmR*, and *mcr11* and *abmR* (Supplemental Figure 2). The promoters of *gyrB* (*Rv0005*) and *efTu* (*Rv0685*) were used as positive controls, and a promoterless construct was used as a negative control. The relevant constructs

were transformed into wild-type (Wt) strains of BCG and Mtb and assayed for β-galactosidase activity in late log phase cultures grown in ambient, shaking conditions by adding 5-acetylaminofluoresceindi-β-D-galactopyranoside (C_2FDG; Molecular Probes) and measuring fluorescence in a Cytofluor 4000 fluorometer (PerSeptive Biosystems) as described previously (95).

Constructs including the *mcr11* promoter, Mcr11 sequence, and various potential intrinsic terminator sequences were fused to the reporter green fluorescent protein Venus (*GFPv*) on an integrating plasmid as previously described (33). A GFPv fluorescence assay was used to measure promoter activity and read-through of the putative intrinsic terminators of Mcr11 in Msm, BCG, and Mtb.

At mid-log phase and late stationary phase, aliquots of recombinant strains were collected and gently sonicated (setting 4, 4 pulses of 5" on time interspersed by 5' off time) using a Virsonic 475 Ultrasonic Cell Disrupter with a cup horn attachment (VirTis Company) before duplicate samples were diluted 1:1 in fresh media. The level of fluorescence in arbitrary units from the GFPv reporter strain was detected using the CytoFluor Multi-Well Plate Reader Series 4000 (PerSeptive Biosystems) at 485 nm excitation and 530 nm emission. The optical density (OD) at 620 nm was read using a Tecan Sunrise® microplate reader and fluorescence levels were normalized to 10^6 bacteria. A promotorless (-) construct was used as a negative control and the promoters P*tuf* and P*gyr* served as positive controls. The % termination was calculated by dividing the observed GFPv fluorescence in arbitrary units of each indicated terminator construct by the

650 amount of GFPv fluorescence in arbitrary units measured from the *mcr11*
651 promoter.

652 Late stationary phase reporter strains of BCG and Mtb were diluted with
653 fresh media to an OD620 nm of 1.25 in a 12 well plate, and then subjected to a
654 variety of cellular stressors for a 24 hour period in shaking, hypoxic conditions
655 (1.3% O_2, 5% CO_2). Cells were treated with 250 μM diethyltriamine-NO (DETA-
656 NO) (Sigma-Aldrich), 1 μg per ml ofloxacin (OFX), 0.28 μg per ml rifampacin
657 (RIF), 53 μg per ml bedaquiline (BDQ), or 0.1% dimethyl sulfoxide (DMSO)
658 vehicle control. GFPv fluorescence in arbitrary units per 106 bacteria (by
659 measured OD at 620 nm) was monitored as described above, and percent
660 termination was calculated relative to P*mcr11* controls.

661 ***Fluorescence-Activated Cell Sorting Analysis***

662 Fluorescence-activated cell sorting analysis was performed on Msm
663 samples that had been fixed with 4% paraformaldehyde (PFA) in phosphate
664 buffered saline (PBS) at pH 7.0 for 30 minutes at room temperature. Fixation was
665 quenched pH-adjusted glycine, and cells were washed three times with PBS.
666 Cells were diluted approximately 1:500 in DPBS and subjected to FACS analysis
667 with a FACS Calibur (Becton Dickson) as previously described (96). Data was
668 collected for 20,000 events per sample and analyzed in CellQuest software
669 (Becton Dickenson).

670 ***RNA Isolation***

671 Total RNA was harvested from Msm, BCG and Mtb after cultures were
672 treated 0.5 M final GTC solution (5.0 M guanadinium isothiocyanate, 25 mM

673 sodium citrate, 0.5% sarkosyl, and 0.1 M 2-β-mercaptoethanol) and pelleted at
674 4°C. Pelleted cells were resuspended in TRIzol Reagent (Invitrogen) and cells
675 were disrupted with 0.1 mm zirconia-silica beads (BioSpec Products) and three
676 70-second high-speed pulse treatments in a bead-beater (BioSpec Products).
677 RNA was recovered from lysates with Direct-zol Mini Prep columns (Zymo) per
678 the manufacturer's protocol. RNA was eluted from the column with nuclease free-
679 water, treated with DNaseI (Qiagen) for 20 minutes at room temperature, and
680 isopropanol precipitated. One μg of total RNA was screened for DNA
681 contamination by PCR using primers KM1309 and KM1310 internal to the sigA
682 ORF. The quality of each RNA sample was assessed by running 1.0 μg of DNA-
683 free RNA on a 0.1% (weight/vol) SDS-agarose gel and visualizing intact 23S,
684 16S, and 5S ribosomal RNA bands after staining with ethidium bromide (Sigma-
685 Aldrich).

686 ***Northern Blots***

687 High quality DNA-free total RNA isolated from Msm, BCG, and Mtb was
688 used for Northern blot analysis of Mcr11 expression. 3-10 μg RNA was separated
689 on a 10% 8 M urea PAGE run at a constant current of 20 mA for 1-1.5 h. The gel
690 was electroblotted onto a Hybond N (Millipore) nylon membrane using a wet
691 transfer system (Bio-Rad Laboratories) as previously described (Girardin, in
692 prep). Blots were UV cross-linked and baked at 80°C for 2 h prior to pre-
693 hybridization at 42°C for 1 h in Rabid-Hyb Buffer (GE Healthcare Life Sciences).
694 Hybridization with α-^{32}P-ATP end-labeled DNA oligo probes was performed at

42°C for 2-16 h. Blots were washed per the manufacturer's protocol and exposed to phosphor-screens for visualization.

Generation of Mycobacterial Cell Lysates and Western Blotting

Strains of BCG and Mtb were grown in the desired condition, and pelleted and washed twice in ice-cold Dulbecco's phosphate buffered saline, calcium and magnesium free (DPBS-CMF), with 0.2% protease inhibitor (Sigma-Aldrich). Cell pellets were resuspended in 1/25 volume lysis buffer (0.3% SDS, 200 mM DTT, 28 mM Tris-Hcl, 22 mM Tris-Base, and 1% protease inhibitor cocktail) and disrupted by two rounds of high-powered sonication at 4°C with Virsonic 475 Ultrasonic Cell Disrupter with a cup horn attachment (VirTis Company) interspersed with 10 freeze-thaw cycles as previously described (33). Lysate was cleared by centrifugation and the cleared lystate was heat-killed at 95°C before quantification with a NanoDrop 2000 (Thermo Scientific).

A total of 30 μg protein of each sample was separated by 12-15% Tris-glycine SDS-PAGE, and gels were immunoblotted on Immobilon-P membranes (Millipore) for 1h at 1 mA/cm^2 using a wet transfer system (Bio-Rad Laboratories). Blots were blocked and proved with 1° antibody in 5% milk (vol/vol) in 50 mM Tris-buffered saline with 0.05% (vol/vol) Tween-20 (Fisher Scientific). Monoclonal antibodies against *Mycobacterium tuberculosis* GlcB (Gene Rv1837c), Clone α-GlcB (produced *in vitro* NR-13799) was obtained through the NIH Biodefense and Emerging Infections Research Resources Repository, NIAID, NIH. Polyclonal mouse AbmR anti-serum was previously generated in-house (33). Polyclonal rabbit anti-lipoic acid antibody (EMD

718 Millipore catalogue # 437695-100ul) was obtained from Fisher Scientific. Primary
719 antibodies were detected with peroxidase conjugated goat secondary antibody
720 and enhanced chemiluminescence (ECL) western blotting detection reagent
721 (Thermo Scientific).

722 ***Growth Curve Analysis***

723 The growth of BCG and Mtb in hypoxic (1.3% O2, 5% CO2), shaking
724 conditions were monitored by measuring the optical density at 620 nm (OD620)
725 of gently sonicated aliquots of cells with a Tecan Sunrise® microplate reader.
726 Cultures were grown in vented T25 tissue culture flasks (Corning), and time
727 points were in single or multi-day intervals. Growth comparisons between
728 Middlebrook 7H9 + 0.2% glycerol, 10% OADC, and 0.05% Tween-80 (+OA) or in
729 Middlebrook 7H9 + 0.2% glycerol, 10% ADC, and 0.05% Tyloxapol (-OA) were
730 made.

731

732 **Acknowledgements**

733 We are very grateful to Dr. Guangchun Bai and Damen Schaak for
734 generating the *mcr11* knockout strains of BCG and Mtb used in this study. We
735 also thank Dr. Joseph Wade for helpful discussions, and gratefully acknowledge
736 the Wadsworth Center Applied Genomics Technologies Core for DNA
737 sequencing and the Wadsworth Center Media and Tissue Culture Core for media
738 preparation.

References

1. WHO. Global Tuberculosis Report 2018. Geneva: World Health Organization, 2018. 2018.
2. Gomez JE, McKinney JD. M. tuberculosis persistence, latency, and drug tolerance. Tuberculosis. 2004;84(1-2):29-44.
3. Bergkessel M, Basta DW, Newman DK. The physiology of growth arrest: uniting molecular and environmental microbiology. Nat Rev Microbiol. 2016;14(9):549-62.
4. Garton NJ, Waddell SJ, Sherratt AL, Lee SM, Smith RJ, Senner C, et al. Cytological and transcript analyses reveal fat and lazy persister-like bacilli in tuberculous sputum. PLoS medicine. 2008;5(4):e75.
5. Honaker RW, Dhiman RK, Narayanasamy P, Crick DC, Voskuil MI. DosS responds to a reduced electron transport system to induce the Mycobacterium tuberculosis DosR regulon. J Bacteriol. 2010;192(24):6447-55.
6. Iona E, Pardini M, Mustazzolu A, Piccaro G, Nisini R, Fattorini L, et al. Mycobacterium tuberculosis gene expression at different stages of hypoxia-induced dormancy and upon resuscitation. Journal of microbiology (Seoul, Korea). 2016;54(8):565-72.
7. Schubert OT, Ludwig C, Kogadeeva M, Zimmermann M, Rosenberger G, Gengenbacher M, et al. Absolute Proteome Composition and Dynamics during Dormancy and Resuscitation of Mycobacterium tuberculosis. Cell Host Microbe. 2015;18(1):96-108.
8. Betts JC, Lukey PT, Robb LC, McAdam RA, Duncan K. Evaluation of a nutrient starvation model of Mycobacterium tuberculosis persistence by gene and protein expression profiling. Molecular Microbiology. 2002;43(3):717-31.
9. Shi L, Sohaskey CD, Kana BD, Dawes S, North RJ, Mizrahi V, et al. Changes in energy metabolism of Mycobacterium tuberculosis in mouse lung and under in vitro conditions affecting aerobic respiration. Proc Natl Acad Sci U S A. 2005;102(43):15629-34.
10. Eoh H, Rhee KY. Methylcitrate cycle defines the bactericidal essentiality of isocitrate lyase for survival of Mycobacterium tuberculosis on fatty acids. Proc Natl Acad Sci U S A. 2014;111(13):4976-81.
11. McKinney JD, Honer zu Bentrup K, Munoz-Elias EJ, Miczak A, Chen B, Chan WT, et al. Persistence of Mycobacterium tuberculosis in macrophages and mice requires the glyoxylate shunt enzyme isocitrate lyase. Nature. 2000;406(6797):735-8.
12. Munoz-Elias EJ, McKinney JD. Mycobacterium tuberculosis isocitrate lyases 1 and 2 are jointly required for in vivo growth and virulence. Nature medicine. 2005;11(6):638-44.
13. Beste DJ, Bonde B, Hawkins N, Ward JL, Beale MH, Noack S, et al. (1)(3)C metabolic flux analysis identifies an unusual route for pyruvate dissimilation in mycobacteria which requires isocitrate lyase and carbon dioxide fixation. PLoS Pathog. 2011;7(7):e1002091.
14. Ganapathy U, Marrero J, Calhoun S, Eoh H, de Carvalho LP, Rhee K, et al. Two enzymes with redundant fructose bisphosphatase activity sustain

785 gluconeogenesis and virulence in Mycobacterium tuberculosis. Nat Commun.
786 2015;6:7912.
787 15. Gutka HJ, Wang Y, Franzblau SG, Movahedzadeh F. glpx Gene in
788 Mycobacterium tuberculosis Is Required for In Vitro Gluconeogenic Growth and
789 In Vivo Survival. PLoS One. 2015;10(9):e0138436.
790 16. Marrero J, Rhee KY, Schnappinger D, Pethe K, Ehrt S. Gluconeogenic
791 carbon flow of tricarboxylic acid cycle intermediates is critical for Mycobacterium
792 tuberculosis to establish and maintain infection. Proc Natl Acad Sci U S A.
793 2010;107(21):9819-24.
794 17. Bryk R, Gold B, Venugopal A, Singh J, Samy R, Pupek K, et al. Selective
795 killing of nonreplicating mycobacteria. Cell Host Microbe. 2008;3(3):137-45.
796 18. Venugopal A, Bryk R, Shi S, Rhee K, Rath P, Schnappinger D, et al.
797 Virulence of Mycobacterium tuberculosis depends on lipoamide dehydrogenase,
798 a member of three multienzyme complexes. Cell Host Microbe. 2011;9(1):21-31.
799 19. Shi S, Ehrt S. Dihydrolipoamide acyltransferase is critical for
800 Mycobacterium tuberculosis pathogenesis. Infect Immun. 2006;74(1):56-63.
801 20. Mvubu NE, Pillay B, Gamieldien J, Bishai W, Pillay M. Canonical
802 pathways, networks and transcriptional factor regulation by clinical strains of
803 Mycobacterium tuberculosis in pulmonary alveolar epithelial cells. Tuberculosis
804 (Edinb). 2016;97:73-85.
805 21. Schnappinger D, Ehrt S, Voskuil MI, Liu Y, Mangan JA, Monahan IM, et al.
806 Transcriptional Adaptation of Mycobacterium tuberculosis within Macrophages:
807 Insights into the Phagosomal Environment. J Exp Med. 2003;198(5):693-704.
808 22. Waters LS, Storz G. Regulatory RNAs in bacteria. Cell. 2009;136(4):615-
809 28.
810 23. Arnvig KB, Young DB. Identification of small RNAs in Mycobacterium
811 tuberculosis. Mol Microbiol. 2009;73(3):397-408.
812 24. DiChiara JM, Contreras-Martinez LM, Livny J, Smith D, McDonough KA,
813 Belfort M. Multiple small RNAs identified in Mycobacterium bovis BCG are also
814 expressed in Mycobacterium tuberculosis and Mycobacterium smegmatis.
815 Nucleic Acids Res. 2010;38(12):4067-78.
816 25. Moores A, Riesco AB, Schwenk S, Arnvig KB. Expression, maturation and
817 turnover of DrrS, an unusually stable, DosR regulated small RNA in
818 Mycobacterium tuberculosis. PLoS One. 2017;12(3):e0174079.
819 26. Pelly S, Bishai WR, Lamichhane G. A screen for non-coding RNA in
820 Mycobacterium tuberculosis reveals a cAMP-responsive RNA that is expressed
821 during infection. Gene. 2012;500(1):85-92.
822 27. Namouchi A, Gomez-Munoz M, Frye SA, Moen LV, Rognes T, Tonjum T,
823 et al. The Mycobacterium tuberculosis transcriptional landscape under genotoxic
824 stress. BMC Genomics. 2016;17(1):791.
825 28. Gerrick ER, Barbier T, Chase MR, Xu R, Francois J, Lin VH, et al. Small
826 RNA profiling in Mycobacterium tuberculosis identifies MrsI as necessary for an
827 anticipatory iron sparing response. Proc Natl Acad Sci U S A.
828 2018;115(25):6464-9.
829 29. Arnvig KB, Comas I, Thomson NR, Houghton J, Boshoff HI, Croucher NJ,
830 et al. Sequence-based analysis uncovers an abundance of non-coding RNA in

the total transcriptome of Mycobacterium tuberculosis. PLoS Pathog. 2011;7(11):e1002342.
30. Miotto P, Forti F, Ambrosi A, Pellin D, Veiga DF, Balazsi G, et al. Genome-wide discovery of small RNAs in Mycobacterium tuberculosis. PLoS One. 2012;7(12):e51950.
31. Tsai CH, Baranowski C, Livny J, McDonough KA, Wade JT, Contreras LM. Identification of novel sRNAs in mycobacterial species. PLoS One. 2013;8(11):e79411.
32. Ignatov DV, Salina EG, Fursov MV, Skvortsov TA, Azhikina TL, Kaprelyants AS. Dormant non-culturable Mycobacterium tuberculosis retains stable low-abundant mRNA. BMC Genomics. 2015;16:954.
33. Girardin RC, Bai G, He J, Sui H, McDonough KA. AbmR (Rv1265) is a Novel Transcription Factor of Mycobacterium tuberculosis That Regulates Host Cell Association and Expression of the Non-coding Small RNA Mcr11. Mol Microbiol. 2018.
34. Dubey AK, Baker CS, Romeo T, Babitzke P. RNA sequence and secondary structure participate in high-affinity CsrA-RNA interaction. RNA. 2005;11(10):1579-87.
35. Hnilicova J, Jirat Matejckova J, Sikova M, Pospisil J, Halada P, Panek J, et al. Ms1, a novel sRNA interacting with the RNA polymerase core in mycobacteria. Nucleic Acids Res. 2014;42(18):11763-76.
36. DeJesus MA, Gerrick ER, Xu W, Park SW, Long JE, Boutte CC, et al. Comprehensive Essentiality Analysis of the Mycobacterium tuberculosis Genome via Saturating Transposon Mutagenesis. MBio. 2017;8(1).
37. Mooney RA, Landick R. Building a better stop sign: understanding the signals that terminate transcription. Nat Methods. 2013;10(7):618-9.
38. Ray-Soni A, Bellecourt MJ, Landick R. Mechanisms of Bacterial Transcription Termination: All Good Things Must End. Annu Rev Biochem. 2016;85:319-47.
39. Santangelo TJ, Artsimovitch I. Termination and antitermination: RNA polymerase runs a stop sign. Nat Rev Microbiol. 2011;9(5):319-29.
40. Peters JM, Mooney RA, Kuan PF, Rowland JL, Keles S, Landick R. Rho directs widespread termination of intragenic and stable RNA transcription. Proc Natl Acad Sci U S A. 2009;106(36):15406-11.
41. Botella L, Vaubourgeix J, Livny J, Schnappinger D. Depleting Mycobacterium tuberculosis of the transcription termination factor Rho causes pervasive transcription and rapid death. Nat Commun. 2017;8:14731.
42. Czyz A, Mooney RA, Iaconi A, Landick R. Mycobacterial RNA polymerase requires a U-tract at intrinsic terminators and is aided by NusG at suboptimal terminators. MBio. 2014;5(2):e00931.
43. Gardner PP, Barquist L, Bateman A, Nawrocki EP, Weinberg Z. RNIE: genome-wide prediction of bacterial intrinsic terminators. Nucleic Acids Res. 2011;39(14):5845-52.
44. Mitra A, Angamuthu K, Nagaraja V. Genome-wide analysis of the intrinsic terminators of transcription across the genus Mycobacterium. Tuberculosis (Edinb). 2008;88(6):566-75.

45. Arnvig KB, Pennell S, Gopal B, Colston MJ. A high-affinity interaction between NusA and the rrn nut site in Mycobacterium tuberculosis. Proc Natl Acad Sci U S A. 2004;101(22):8325-30.
46. Mathews DH. RNA Secondary Structure Analysis Using RNAstructure. Current Protocols in Bioinformatics: John Wiley & Sons, Inc.; 2002.
47. Morita T, Ueda M, Kubo K, Aiba H. Insights into transcription termination of Hfq-binding sRNAs of Escherichia coli and characterization of readthrough products. RNA. 2015;21(8):1490-501.
48. Tjaden B. TargetRNA: a tool for predicting targets of small RNA action in bacteria. Nucleic Acids Res. 2008;36(Web Server issue):W109-13.
49. Kery MB, Feldman M, Livny J, Tjaden B. TargetRNA2: identifying targets of small regulatory RNAs in bacteria. Nucleic Acids Res. 2014;42(Web Server issue):W124-9.
50. Cortes T, Schubert OT, Rose G, Arnvig KB, Comas I, Aebersold R, et al. Genome-wide mapping of transcriptional start sites defines an extensive leaderless transcriptome in Mycobacterium tuberculosis. Cell Rep. 2013;5(4):1121-31.
51. Gazdik MA, Bai G, Wu Y, McDonough KA. Rv1675c (cmr) regulates intramacrophage and cyclic AMP-induced gene expression in Mycobacterium tuberculosis-complex mycobacteria. Mol Microbiol. 2009;71(2):434-48.
52. Spalding MD, Prigge ST. Lipoic acid metabolism in microbial pathogens. Microbiol Mol Biol Rev. 2010;74(2):200-28.
53. Bazet Lyonnet B, Diacovich L, Cabruja M, Bardou F, Quemard A, Gago G, et al. Pleiotropic effect of AccD5 and AccE5 depletion in acyl-coenzyme A carboxylase activity and in lipid biosynthesis in mycobacteria. PLoS One. 2014;9(6):e99853.
54. Bazet Lyonnet B, Diacovich L, Gago G, Spina L, Bardou F, Lemassu A, et al. Functional reconstitution of the Mycobacterium tuberculosis long-chain acyl-CoA carboxylase from multiple acyl-CoA subunits. FEBS J. 2017;284(7):1110-25.
55. Sassetti CM, Boyd DH, Rubin EJ. Genes required for mycobacterial growth defined by high density mutagenesis. Molecular Microbiology. 2003;48(1):77-84.
56. Sassetti CM, Rubin EJ. Genetic requirements for mycobacterial survival during infection. Proc Natl Acad Sci U S A. 2003;100(22):12989-94.
57. Chae H, Han K, Kim KS, Park H, Lee J, Lee Y. Rho-dependent termination of ssrS (6S RNA) transcription in Escherichia coli: implication for 3' processing of 6S RNA and expression of downstream ygfA (putative 5-formyl-tetrahydrofolate cyclo-ligase). J Biol Chem. 2011;286(1):114-22.
58. Kriner MA, Sevostyanova A, Groisman EA. Learning from the Leaders: Gene Regulation by the Transcription Termination Factor Rho. Trends in biochemical sciences. 2016;41(8):690-9.
59. Patrick R. Shiflett KJT-M, Ryszard Michalczyk, Louis A. “Pete” Silks, and Goutam Gupta. Structural Studies on the Hairpins at the 3' Untranslated Region of an Anthrax Toxin Gene. Biochemistry 2003;42(20):6078-89.

60. Ishikawa H, Otaka H, Maki K, Morita T, Aiba H. The functional Hfq-binding module of bacterial sRNAs consists of a double or single hairpin preceded by a U-rich sequence and followed by a 3' poly(U) tail. RNA. 2012;18(5):1062-74.
61. Johnson CM, Chen Y, Lee H, Ke A, Weaver KE, Dunny GM. Identification of a conserved branched RNA structure that functions as a factor-independent terminator. Proc Natl Acad Sci U S A. 2014;111(9):3573-8.
62. Regnier P, Hajnsdorf E. The interplay of Hfq, poly(A) polymerase I and exoribonucleases at the 3' ends of RNAs resulting from Rho-independent termination: A tentative model. RNA Biol. 2013;10(4):602-9.
63. Sauer E, Weichenrieder O. Structural basis for RNA 3'-end recognition by Hfq. Proc Natl Acad Sci U S A. 2011;108(32):13065-70.
64. Olejniczak M, Storz G. ProQ/FinO-domain proteins: another ubiquitous family of RNA matchmakers? Mol Microbiol. 2017;104(6):905-15.
65. Rabhi M, Espeli O, Schwartz A, Cayrol B, Rahmouni AR, Arluison V, et al. The Sm-like RNA chaperone Hfq mediates transcription antitermination at Rho-dependent terminators. EMBO J. 2011;30(14):2805-16.
66. Agrawal A, Mohanty BK, Kushner SR. Processing of the seven valine tRNAs in Escherichia coli involves novel features of RNase P. Nucleic Acids Res. 2014;42(17):11166-79.
67. Chao Y, Li L, Girodat D, Forstner KU, Said N, Corcoran C, et al. In Vivo Cleavage Map Illuminates the Central Role of RNase E in Coding and Non-coding RNA Pathways. Mol Cell. 2017;65(1):39-51.
68. Gopel Y, Khan MA, Gorke B. Domain swapping between homologous bacterial small RNAs dissects processing and Hfq binding determinants and uncovers an aptamer for conditional RNase E cleavage. Nucleic Acids Res. 2016;44(2):824-37.
69. Mohanty BK, Kushner SR. Processing of the Escherichia coli leuX tRNA transcript, encoding tRNA(Leu5), requires either the 3'-->5' exoribonuclease polynucleotide phosphorylase or RNase P to remove the Rho-independent transcription terminator. Nucleic Acids Res. 2010;38(2):597-607.
70. Mohanty BK, Petree JR, Kushner SR. Endonucleolytic cleavages by RNase E generate the mature 3' termini of the three proline tRNAs in Escherichia coli. Nucleic Acids Res. 2016;44(13):6350-62.
71. Dar D, Sorek R. High-resolution RNA 3'-ends mapping of bacterial Rho-dependent transcripts. Nucleic Acids Res. 2018;46(13):6797-805.
72. Abendroth J, Ollodart A, Andrews ES, Myler PJ, Staker BL, Edwards TE, et al. Mycobacterium tuberculosis Rv2179c protein establishes a new exoribonuclease family with broad phylogenetic distribution. J Biol Chem. 2014;289(4):2139-47.
73. Taverniti V, Forti F, Ghisotti D, Putzer H. Mycobacterium smegmatis RNase J is a 5'-3' exo-/endoribonuclease and both RNase J and RNase E are involved in ribosomal RNA maturation. Mol Microbiol. 2011;82(5):1260-76.
74. Uson ML, Ordonez H, Shuman S. Mycobacterium smegmatis HelY Is an RNA-Activated ATPase/dATPase and 3'-to-5' Helicase That Unwinds 3'-Tailed RNA Duplexes and RNA:DNA Hybrids. J Bacteriol. 2015;197(19):3057-65.

75. Zeller ME, Csanadi A, Miczak A, Rose T, Bizebard T, Kaberdin VR. Quaternary structure and biochemical properties of mycobacterial RNase E/G. The Biochemical journal. 2007;403(1):207-15.
76. Zhu L, Phadtare S, Nariya H, Ouyang M, Husson RN, Inouye M. The mRNA interferases, MazF-mt3 and MazF-mt7 from Mycobacterium tuberculosis target unique pentad sequences in single-stranded RNA. Mol Microbiol. 2008;69(3):559-69.
77. Zhu L, Zhang Y, Teh JS, Zhang J, Connell N, Rubin H, et al. Characterization of mRNA interferases from Mycobacterium tuberculosis. J Biol Chem. 2006;281(27):18638-43.
78. Vandal OH, Pierini LM, Schnappinger D, Nathan CF, Ehrt S. A membrane protein preserves intrabacterial pH in intraphagosomal Mycobacterium tuberculosis. Nature medicine. 2008;14(8):849-54.
79. Lofthouse EK, Wheeler PR, Beste DJ, Khatri BL, Wu H, Mendum TA, et al. Systems-based approaches to probing metabolic variation within the Mycobacterium tuberculosis complex. PLoS One. 2013;8(9):e75913.
80. Schaefer WB, Lewis CW, Jr. Effect of oleic acid on growth and cell structure of mycobacteria. J Bacteriol. 1965;90(5):1438-47.
81. Griffin JE, Gawronski JD, Dejesus MA, Ioerger TR, Akerley BJ, Sassetti CM. High-resolution phenotypic profiling defines genes essential for mycobacterial growth and cholesterol catabolism. PLoS Pathog. 2011;7(9):e1002251.
82. Hamoen LW. Cell division blockage: but this time by a surprisingly conserved protein. Mol Microbiol. 2011;81(1):1-3.
83. Tchigvintsev A, Tchigvintsev D, Flick R, Popovic A, Dong A, Xu X, et al. Biochemical and Structural Studies of Conserved Maf Proteins Revealed Nucleotide Pyrophosphatases with a Preference for Modified Nucleotides. Chemistry & Biology. 2013;20(11):1386-98.
84. Gago G, Kurth D, Diacovich L, Tsai SC, Gramajo H. Biochemical and structural characterization of an essential acyl coenzyme A carboxylase from Mycobacterium tuberculosis. J Bacteriol. 2006;188(2):477-86.
85. Desnoyers G, Morissette A, Prevost K, Masse E. Small RNA-induced differential degradation of the polycistronic mRNA iscRSUA. EMBO J. 2009;28(11):1551-61.
86. Florczyk MA, McCue LA, Stack RF, Hauer CR, McDonough KA. Identification and characterization of mycobacterial proteins differentially expressed under standing and shaking culture conditions, including Rv2623 from a novel class of putative ATP-binding proteins. Infect Immun. 2001;69(9):5777-85.
87. Bardarov S, Bardarov Jr S, Jr., Pavelka Jr MS, Jr., Sambandamurthy V, Larsen M, Tufariello J, et al. Specialized transduction: an efficient method for generating marked and unmarked targeted gene disruptions in Mycobacterium tuberculosis, M. bovis BCG and M. smegmatis. Microbiology. 2002;148(Pt 10):3007-17.

88. Beauregard A, Smith EA, Petrone BL, Singh N, Karch C, McDonough KA, et al. Identification and characterization of small RNAs in Yersinia pestis. RNA Biol. 2013;10(3):397-405.
89. Darty K, Denise A, Ponty Y. VARNA: Interactive drawing and editing of the RNA secondary structure. Bioinformatics. 2009;25(15):1974-5.
90. Huff J, Czyz A, Landick R, Niederweis M. Taking phage integration to the next level as a genetic tool for mycobacteria. Gene. 2010;468(1-2):8-19.
91. Ding Y, Chan CY, Lawrence CE. Sfold web server for statistical folding and rational design of nucleic acids. Nucleic Acids Res. 2004;32(Web Server issue):W135-41.
92. Zadeh JN, Steenberg CD, Bois JS, Wolfe BR, Pierce MB, Khan AR, et al. NUPACK: Analysis and design of nucleic acid systems. J Comput Chem. 2011;32(1):170-3.
93. Zuker M. Mfold web server for nucleic acid folding and hybridization prediction. Nucleic Acids Research. 2003;31(13):3406-15.
94. Sato K, Hamada M, Asai K, Mituyama T. CENTROIDFOLD: a web server for RNA secondary structure prediction. Nucleic Acids Res. 2009;37(Web Server issue):W277-80.
95. Vasudeva-Rao HM, McDonough KA. Expression of the Mycobacterium tuberculosis acr-coregulated genes from the DevR (DosR) regulon is controlled by multiple levels of regulation. Infect Immun. 2008;76(6):2478-89.
96. Purkayastha A, McCue LA, McDonough KA. Identification of a Mycobacterium tuberculosis Putative Classical Nitroreductase Gene Whose Expression Is Coregulated with That of the acr Gene within Macrophages, in Standing versus Shaking Cultures, and under Low Oxygen Conditions. Infection and Immunity. 2002;70(3):1518-29.

Figure Legends

Figure 1. Secondary Structure modeling of 3' sequences beyond the mapped 3' end of Mcr11. A. The DNA sequence of the *mcr11* gene and extended 3' sequence used for modeling experiments is shown. The *mcr11* gene is shown in capital letters, and nucleotides where 5' and 3' boundaries have been mapped by RACE are indicated by arrows and shown in capitalized, bolded black text. Flanking sequences are in italics, and the Rv1264 stop codon in bolded in red text. The last nucleotide on the 3' side of mcr11 that was included in modeling experiments is in bold, lowercase black text. An asterisk indicates 3' ends reported by DiChiara et al and DeJesus et al. Positions of mapped nucleotides on the Mtb chromosome are shown above the text. B. Secondary structure diagrams of Mcr11 from 5' position 1413227 and extended 3' native sequences. The synthetic idealized intrinsic termination control ($tt_{sbi}B$) is also modeled onto Mcr11 from the longest 3' end reported at position 1413094; the last nucleotide of native sequence 3' to Mcr11 is indicated by a black arrow. Black nucleotides indicate bases in the mapped boundaries of the *mcr11* gene, red base pairs indicate base pairs beyond the mapped 3' end of Mcr11 at position 1413107, except all uracils (Us) are shown in blue. An asterisk indicates that last nucleotide modeled in (C.). C. The secondary structure models with the lowest minimum free energies (MFE) of a shorter untested native Mcr11 TSE with the most U rich sequence at the 3' end of the putative terminator. The MFE of each structure is shown below each diagram.

Figure 2. TSEs decrease transcriptional read-through of Mcr11-GFPv reporters, but Mcr11 is not robustly expressed in Msm, even in the presence of *abmR* from Mtb. A. A schematic representation of GFPv fluorescence-based reporter assay to determine the functionality of TSEs, and a synthetic idealized intrinsic termination control ($tt_{sbi}B$). B. GFPv fluorescence assay used to measure promoter activity and read-through of TSEs of *mcr11* in late stationary phase Msm, which lacks a native *mcr11* locus. The promoter P*tuf* served as a positive control. The various TSE constructs tested are indicated underneath the corresponding bar. Statistical comparisons are relative to P*mcr11*. C. The % termination of constructs tested in (B.). Statistical comparisons are relative to TSE1. D. Northern blot analysis of Mcr11 expression (M) in Msm with various *mcr11* + TSE constructs. Ten ug of total Msm RNA was loaded, whereas 3 ug of the BCG positive control was loaded. The HisT tRNA (H) was used as a loading control. E. GFPv fluorescence assay used to measure promoter activity in Msm. Statistical comparisons are relative to P*mcr11* or between 24h and 28h as indicated. Results are the means of 3 biological replicates. Statistical analysis conducted with an unpaired, 2-tailed Student's t-test. Asterisks indicate significance as follows: * $p<0.05$, ** $p<0.01$, *** $p<0.001$, **** $p<0.0001$.

Figure 3. Efficiency of TSEs are positively regulated in response to growth phase in BCG and function significantly better in Mtb. A. GFPv fluorescence assay used to measure promoter activity and read-through of the TSEs of *mcr11*

in mid-log phase BCG in hypoxic (1.3% O_2, 5% CO_2), shaking conditions. A promoterless (-) construct was used as a negative control and the promoters P*tuf* and P*gyr* served as positive controls. The various TSE constructs tested are indicated underneath the corresponding bar. Statistical comparisons were made to P*mcr11*. B. As in (A), but assayed in late stationary phase. C. A comparison of % termination observed in mid-log phase (solid bars) and late stationary phase (hatched bars) BCG. Statistical comparisons were made between mid-log and stationary phase. D. GFPv fluorescence assay used to measure promoter activity and read-through of the TSEs of *mcr11* in mid-log phase Mtb in hypoxic (1.3% O_2, 5% CO_2), shaking conditions. A promoterless (-) construct was used as a negative control and the promoters P*tuf* and P*gyr* serve as positive controls. The various TSE constructs tested are indicated underneath the corresponding bar. Statistical comparisons are made to P*mcr11*. E. As in (D), but assayed in late stationary phase. Statistical comparisons are made to P*mcr11*. F. A comparison of % termination observed in late stationary phase Msm, BCG, and Mtb. Statistical comparisons are made to Mtb. Results are the means of 3 biological replicates. Statistical analysis conducted with an unpaired, 2-tailed Student's t-test. Asterisks indicate significance as follows: * $p<0.05$, ** $p<0.01$, *** $p<0.001$, **** $p<0.0001$.

Figure 4. Different Mcr11 TSEs do not alter the size of stable Mcr11. A. Northern blot analysis of Mcr11 expression in the indicated strains of BCG in hypoxic (1.3% O_2, 5% CO_2) late stationary phase. B. Northern blot analysis of

Mcr11 expression in the indicated strains of Mtb in hypoxic late stationary phase. The tRNA HisT is used as a loading control. Results representative of 2-3 independent repeats.

Figure 5. Termination at a sub-optimal TSE does not require a trans-gene for stabilization of Mcr11. A. A schematic of the transgene fusion constructs. *Mcr11* complementation was provided with (1) or without (2) the transgene GFPv fused to the end of *mcr11* downstream of sub-optimal terminator TSE1. An Mcr11 complementation construct was also tested with TSE3 (3). B. Northern blot analysis of Mcr11 expression in Mtb grown to late stationary phase in hypoxia (1.3% O_2, 5% CO_2). HisT was used as a loading control. C. Northern blot analysis Mcr11 expression across growth phase in BCG, indicated below. HisT was used as a loading control. D. qPCR analysis of Mcr11 expression in mid-log and late stationary phase BCG, normalized to *sigA* expression. Results are the representative of 2-3 biological replicates. Statistical analysis conducted with an unpaired, 2-tailed Student's t-test. Asterisks indicate significance as follows: ** $p<0.01$, *** $p<0.001$.

Figure 6. *Δmcr11* has a disrupted *abmR* promoter, resulting in reduced expression of AbmR protein in BCG and Mtb. A. The *mcr11* locus with the position of the hygromycin knockout cassette is shown. The regions of DNA used to create *promoter:lacZ* fusions are shown. Fragment (1.) includes the *Rv1264-abmR* intergenic region, which includes the *mcr11* locus. Fragment (2.) includes

1131 the *mcr11-Rv1265* sequence that is available in the *Δmcr11* strain. B.
1132 Quantification of western blot analysis from BCG grown to late-log phase in
1133 ambient, shaking conditions. C. Quantification of western blot analysis from Mtb
1134 grown to late-log phase in hypoxic (1.3% O_2, 5% CO_2), shaking conditions.
1135 AbmR was detected with poly-clonal anti-sera, and levels were normalized to
1136 GlcB levels, as detected by a monoclonal antibody. D. β-Galactosidase activity
1137 assays using the promoter:*lacZ* fusions shown in (A.) in Wt BCG (gray bars) and
1138 MTB (black bars) grown to late-log phase in ambient, shaking conditions. An
1139 asterisk * indicates p-value < 0.05 using an unpaired Student's t-test. Results
1140 representative of 2-3 biological repeats.
1141
1142 **Figure 7. Bioinformatic modeling of Mcr11 targets reveals potential**
1143 **regulatory targets that are involved in central metabolism and cell division.**
1144 A. The organization of the *dlaT-lipB* locus, with the position and potential base-
1145 pairing interactions between the mRNA and Mcr11 shown below. The
1146 transcriptional start site of the operon is shown with a thin black arrow. B. As in
1147 (A.), but for the *accD5-Rv3282* locus. Dashes indicate Watson-Crick base pairs,
1148 dots indicate non-Watson-Crick base pairs, and a blank space indicates no
1149 interaction between bases. C. The sequence of the Mcr11 RNA with mapped 5'
1150 and 3' ends shown in bolded letters. The portion of the sRNA predicted to
1151 interact with targets shown in (A) and (B) is underlined in black. D. The MFE
1152 secondary structure of Mcr11 as predicted by RNAStructure, with the portion of
1153 the sRNA predicted to interact with targets shown in (A) and (B) outlined in black.

Figure 8. *Δmcr11* strains of BCG and Mtb are defective for growth in fatty-acid depleted media and predicted regulatory targets of Mcr11 are dysregulated at the mRNA level. A. Mtb was grown for 12 days in under hypoxic (1.3% O_2, 5% CO_2), shaking conditions in -OA media (7H9 + 0.2% glycerol, 10% ADC, and 0.05% Tyloxapol). Gene expression was measured by qRT-PCR and normalized to the reference gene *sigA*. Comparison made of each strain versus *Δmcr11*. Complementation strains included a single-copy of *mcr11* with TSE3 fused to *GFPv* or a single-copy of the *abmR* locus and *mcr11* with TSE4. B. Mtb was grown for 7 days in under hypoxic, shaking conditions in +OA media (7H9 + 0.2% glycerol, 10% OADC, and 0.05% Tyloxapol). Gene expression was measured by qRT-PCR and normalized to the reference gene *sigA*. C. BCG was grown for 12 days in under hypoxic, shaking conditions in -OA media. Gene expression was measured by qRT-PCR and normalized to the reference gene *sigA*. D. BCG was grown for 12 days in under hypoxic, shaking conditions in +OA media. Gene expression was measured by qRT-PCR and normalized to the reference gene *sigA*. E. Growth curve of Mtb grown in hypoxic, shaking conditions in -OA media. Growth was surveyed by measuring the optical density at 620 nm (OD_{620}). F. Growth curve of Mtb grown in hypoxic, shaking conditions in +OA media. Growth was surveyed by measuring OD_{620}. G. As in (E.), but with BCG. H. As in (F.), but with BCG. Results are the means of 3 biological replicates. Statistical comparisons made of each strain versus *Δmcr11* using an unpaired, 2-tailed Student's t-test. Asterisks indicate significance as follows: * $p<0.05$, ** $p<0.01$, *** $p<0.001$, **** $p<0.0001$.

Figure 9. Model of Mcr11 function in Mtb.

Expression of mcr11 is activated by cAMP, chronic infection in the lungs of mice, and by advancing growth phase and the ATP-binding transcription factor AbmR Native 3' sequence elements (TSEs, predicted secondary structure shown in red) promote the transcriptional termination and stability of Mcr11. The predicted secondary structure of mature Mcr11 is shown in black. Mcr11 regulates the expression of genes involved in the central metabolism and growth of Mtb, possibly through a base-pairing interaction between Mcr11 and target mRNAs. Mcr11 is required for the optimal growth of Mtb in the absence of fatty acids

Supporting information

S1 Figure. Generation and confirmation of *mcr11* knock-out and complementation strains. A. A diagram of the *mcr11* locus and the relative position of the hygromycin resistance cassette. Lines with arrows indicated the DNA sequence included in the various listed complementation strains. B. PCR confirmation of *mcr11* knockout and complementation strains of BCG. C. PCR confirmation of *mcr11* knockout and complementation strains of Mtb. D. Northern blot analysis of the indicated strains of BCG from 3 μg of total RNA harvested from late stationary phase cultures grown in hypoxic (1.3% O_2, 5% CO_2), shaking conditions. E. Northern blot analysis of the indicated strains of Mtb from 5 μg of total RNA harvested from late-log phase cultures grown in hypoxic (1.3% O_2, 5% CO_2), shaking conditions. The number above the lane indicates the identity of each sample. The column to the left of the rows indicates which gene was amplified or which RNA was probed by Northern blot.

S2 Figure. FACS analysis of TSEs in Msm. FACS analysis of GFPv fluorescence of 20,000 events for each sample as indicated by the label to the left of the histogram. Representative of three independent repeats.

S3 Figure. *abmR* contributes to the termination of Mcr11 transcripts. A. GFPv fluorescence assay used to measure m*cr11* promoter activity in mid-log phase Mtb in hypoxic (1.3% O_2, 5% CO_2), shaking conditions. B. The % termination in mid-log phase. The various TSE constructs tested are indicated underneath the corresponding bar. C. Promoter reporter assay as in (A), but in late stationary phase. D. The % termination, as in (B), but in late stationary

phase. Results representative of 3 biological replicates. Statistical analysis conducted with an unpaired, 2-tailed Student's t-test. Comparison made versus Mtb*ΔabmR* in A. and C., and versus Wt in B. and D. Asterisks indicate significance as follows: * $p<0.05$, ** $p<0.01$, *** $p<0.001$, **** $p<0.0001$.

S4 Figure. Secondary structure of Mcr11 RNA generated by multiple modeling algorithms. A. The CentroidFold secondary structure using the CONTRAfold inference engine. B. The -54.40 kcal/mol MFE structure generated using Mfold. C. The -45.40 kcal/mol MFE strcture generated using NUPACK. D. The RNAfold centroid structure. E. The -54.00 kcal/mol MFE structure generated using RNAfold. F. The -53.80 kcal/mol MFE structure generated using RNAStructure. G. The ensemble centroid structure generated using Sfold. H. The -54.40 kcal/mol MFE structure generated using Sfold.

S5 Figure. Protein levels of predicted regulatory targets of Mcr11 are not dysregulated in Mtb*Δmcr11* during hypoxia in the absence of added fatty acids. A. Mtb was grown for 12 days in under hypoxic, shaking conditions in -OA media. Gene expression was measured by qRT-PCR and normalized to the reference gene *sigA*. Comparison made of each strain versus Mtb*Δmcr11*. B. Mtb was grown for 12 days in under hypoxic (1.3% O_2, 5% CO_2), shaking conditions in Middlebrook 7H9 + 0.2% glycerol, 10% ADC, and 0.05% Tyloxapol (-OA) media. Protein levels were assayed by Western blot analysis with polyclonal α-Lipoate, polyclonal α-PknA, and monoclonal α-GlcB antibodies. GlcB serves as a loading and transfer control. Representative of three biological repeats.

S6 Figure. Regulation of predicted targets of Mcr11 is condition specific in BCG and Mtb. A. BCG grown for 12 days in under hypoxic (1.3% O_2, 5% CO_2), shaking conditions in Middlebrook 7H9 + 0.2% glycerol, 10% OADC, and 0.05% Tyloxapol (+OA). Gene expression was measured by qRT-PCR and normalized to the reference gene sigA. G.-H. Mtb was grown for 7 days in under hypoxic (1.3% O_2, 5% CO_2), shaking conditions in Middlebrook 7H9 + 0.2% glycerol, 10% OADC, and 0.05% Tween (+OA) and treated with vehicle control (Control) or 10 mM dibutyryl cAMP on day 3 (+db cAMP). Gene expression was measured by qRT-PCR and normalized to the reference gene *sigA*. Representative of 2-3 biological repeats. Statistical analysis conducted with an unpaired, 2-tailed Student's t-test. Comparison made of each strain versus *Δmcr11*. Asterisks indicate significance as follows: * $p<0.05$, ** $p<0.01$, *** $p<0.001$, **** $p<0.0001$.

S1 Table. Plasmids used in the study.

S2 Table. Primers used in the study.

S3 Table. Stress does not impact the efficiency of TSEs in BCG or Mtb.

S4 Table. Results of TargetRNA and TargetRNA2 predictions of Mcr11 regulatory targets.

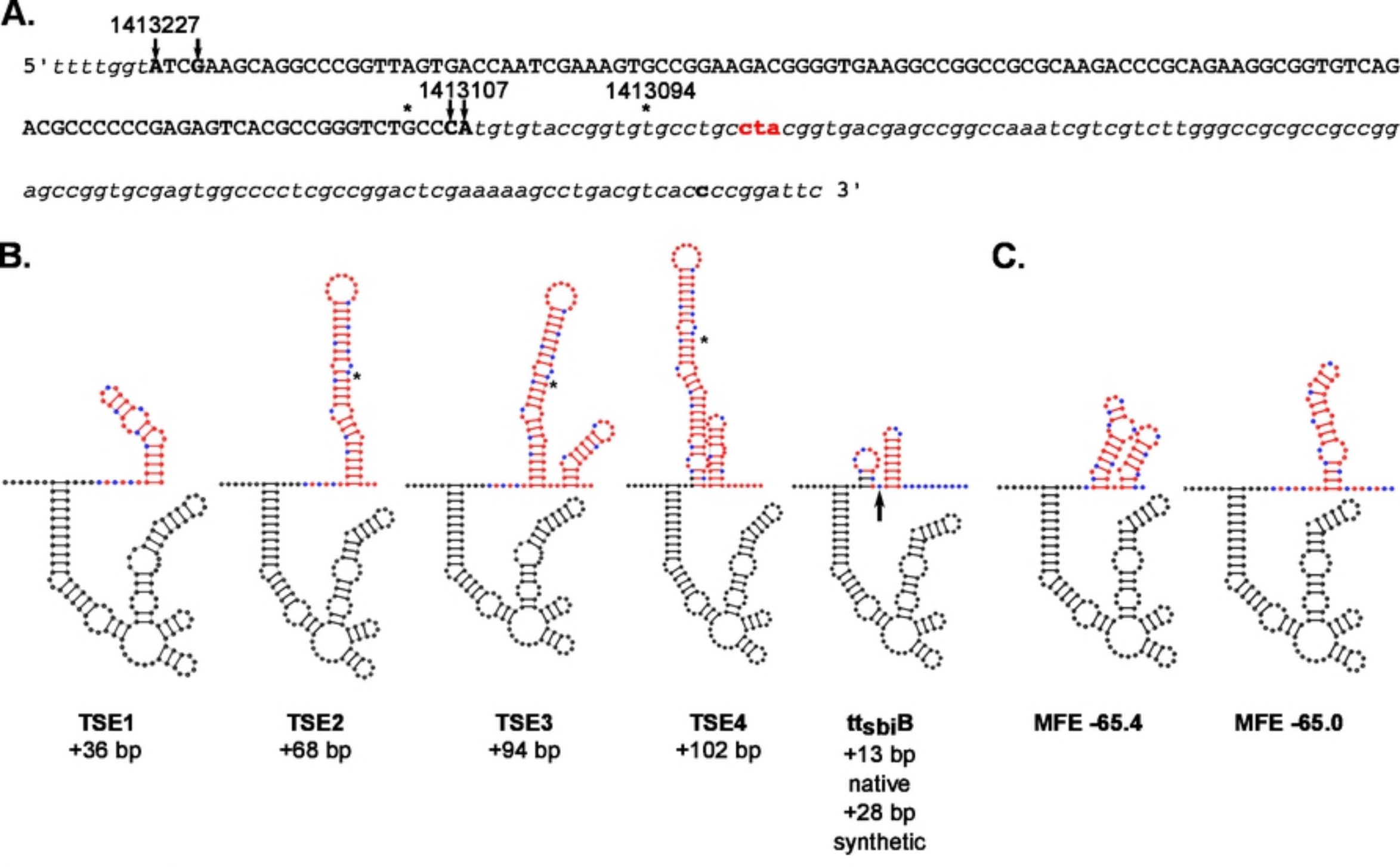
A.
1413227
5' ttttggtATCGAAGCAGGCCCGGTTAGTGACCAATCGAAAGTGCCGGAAGACGGGGTGAAGGCCGGCCGCGCAAGACCCGCAGAAGGCGGTGTCAG
1413107
1413094
ACGCCCCCCGAGAGTCACGCCGGGTCTGCCCAtgtgtaccggtgtgcctgcctacggtgacgagccggccaaatcgtcgtcttgggccgcgccgccgg
agccggtgcgagtggcccctcgccggactcgaaaaagcctgacgtcaccccggattc 3'
B.
C.
TSE1
+36 bp
TSE2
+68 bp
TSE3
+94 bp
TSE4
+102 bp
ttsbiB
+13 bp
native
+28 bp
synthetic
MFE -65.4
MFE -65.0

Figure 1

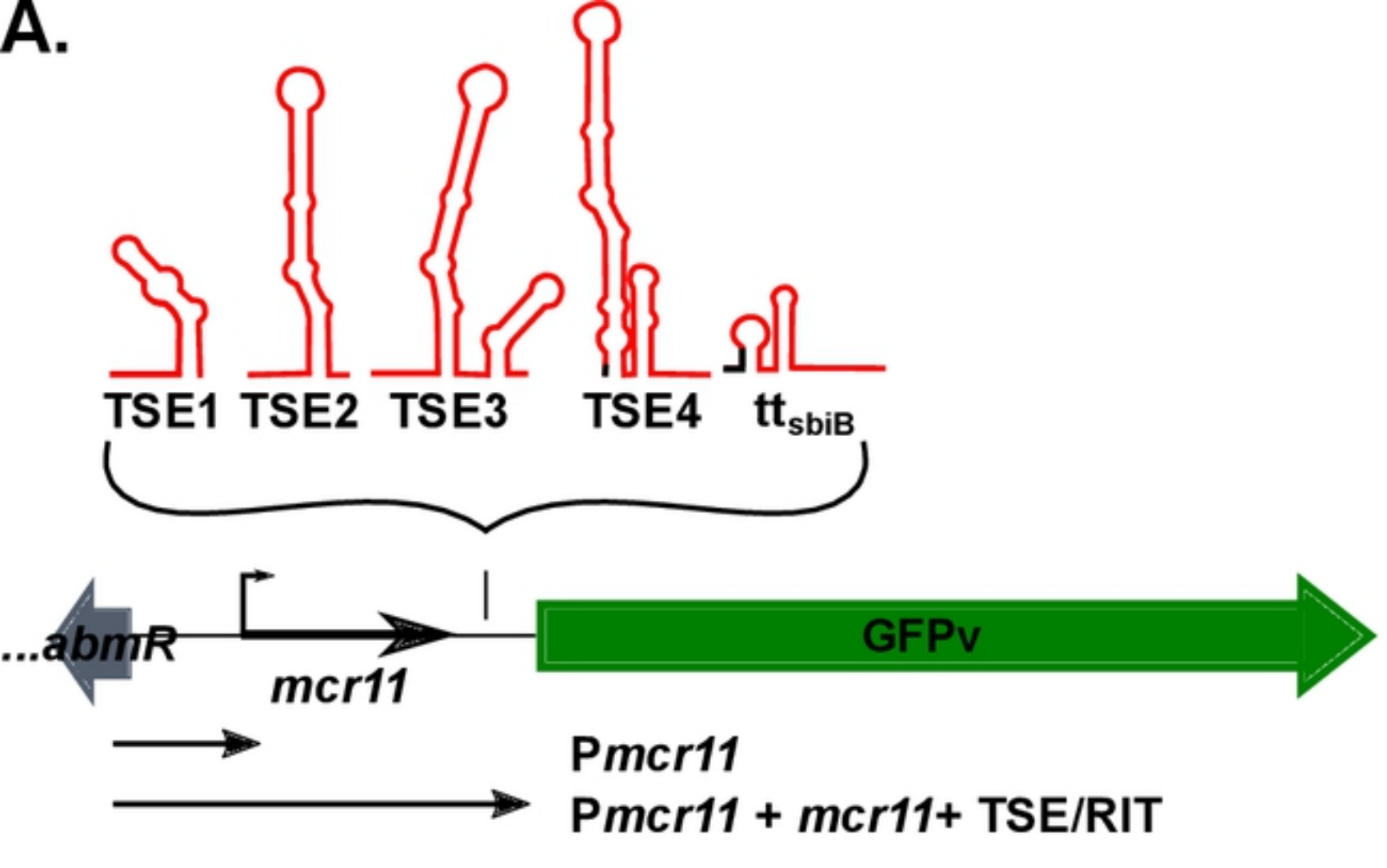

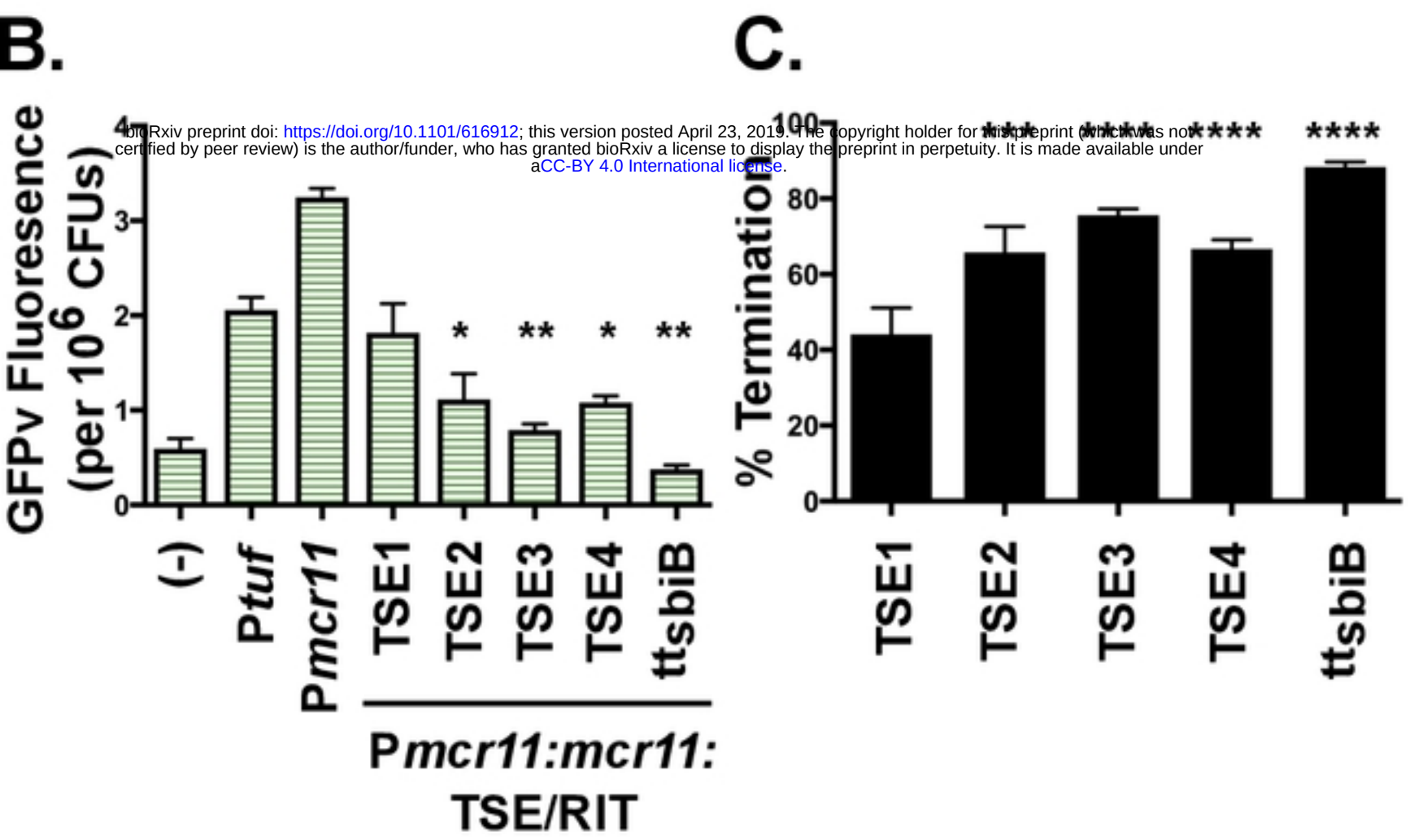

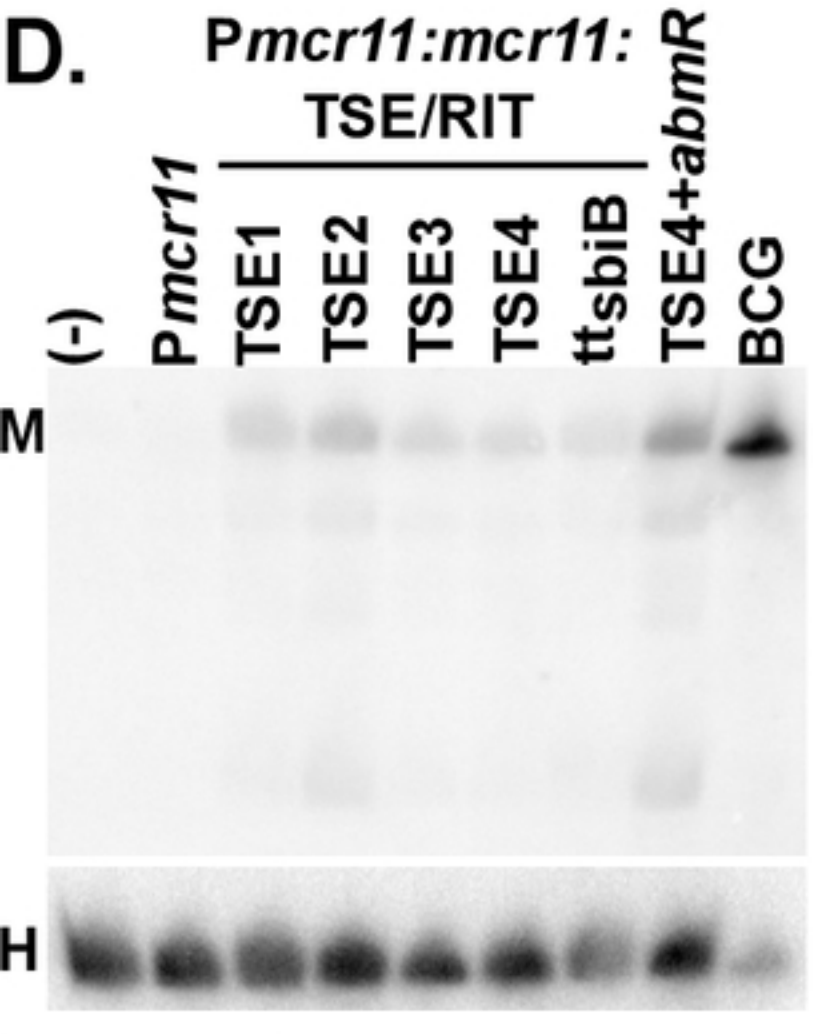

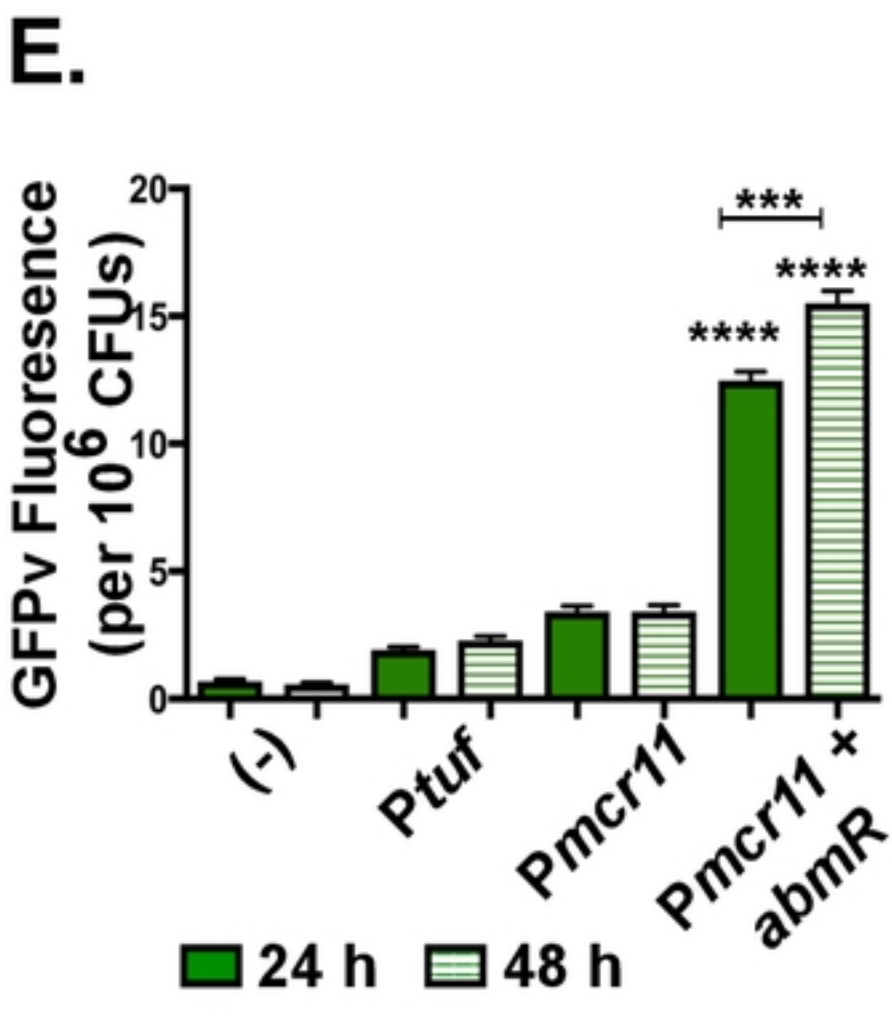

Figure 2

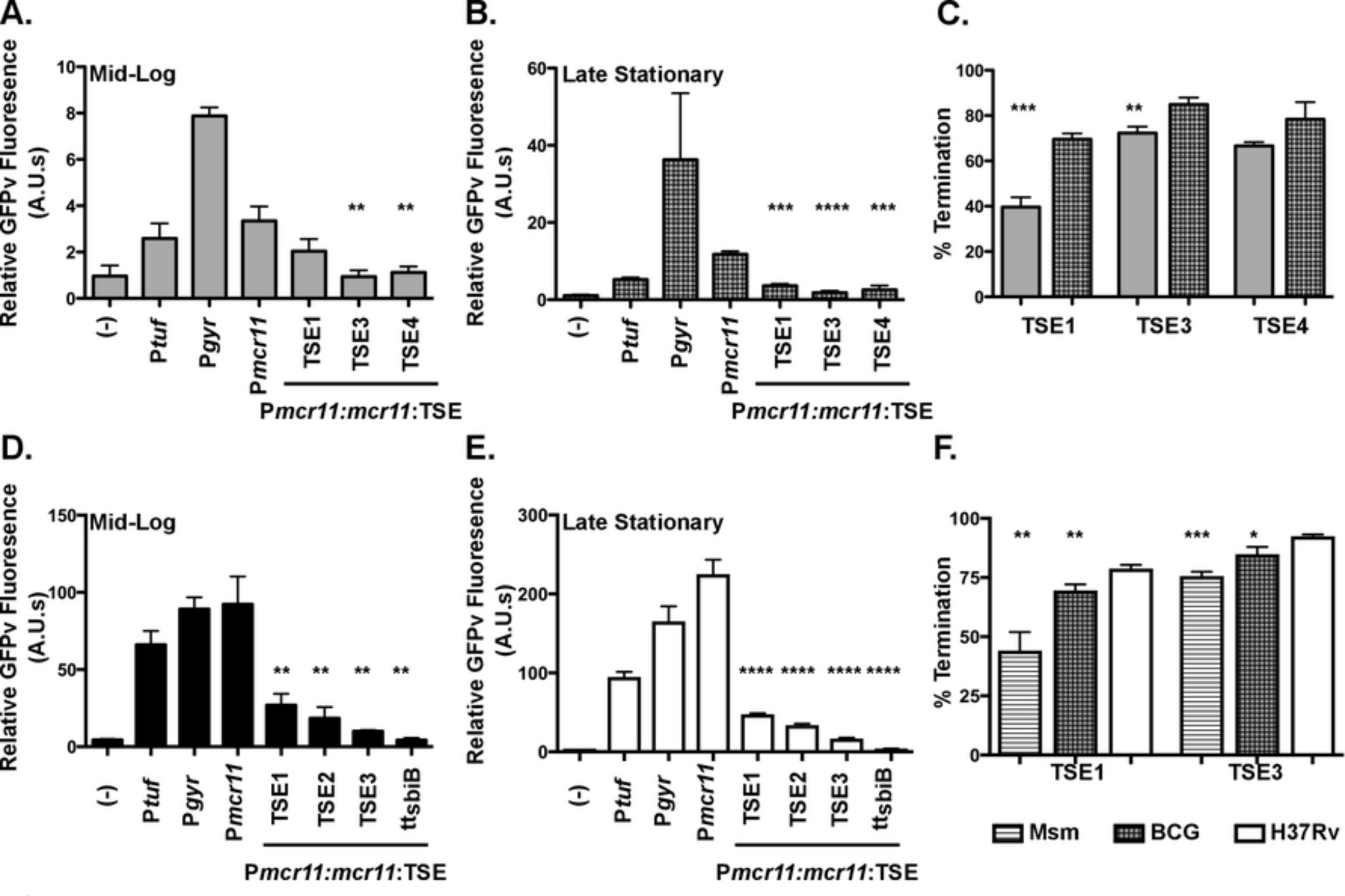
A.
Mid-Log
Relative GFPv Fluorescence (A.U.s)
10
8
6
4
2
0
**
**
(-)
Ptuf
Pgyr
Pmcr11
TSE1
TSE3
TSE4
Pmcr11:mcr11:TSE
B.
Late Stationary
Relative GFPv Fluorescence (A.U.s)
60
40
20
0
***
****
***
(-)
Ptuf
Pgyr
Pmcr11
TSE1
TSE3
TSE4
Pmcr11:mcr11:TSE
C.
% Termination
100
80
60
40
20
0
***
**
TSE1
TSE3
TSE4
D.
Mid-Log
Relative GFPv Fluorescence (A.U.s)
150
100
50
0
**
**
**
**
(-)
Ptuf
Pgyr
Pmcr11
TSE1
TSE2
TSE3
ttsbiB
Pmcr11:mcr11:TSE
E.
Late Stationary
Relative GFPv Fluorescence (A.U.s)
300
200
100
0
****
****
****
****
(-)
Ptuf
Pgyr
Pmcr11
TSE1
TSE2
TSE3
ttsbiB
Pmcr11:mcr11:TSE
F.
% Termination
100
75
50
25
0
**
**
***
*
TSE1
TSE3
Msm
BCG
H37Rv

Figure 3

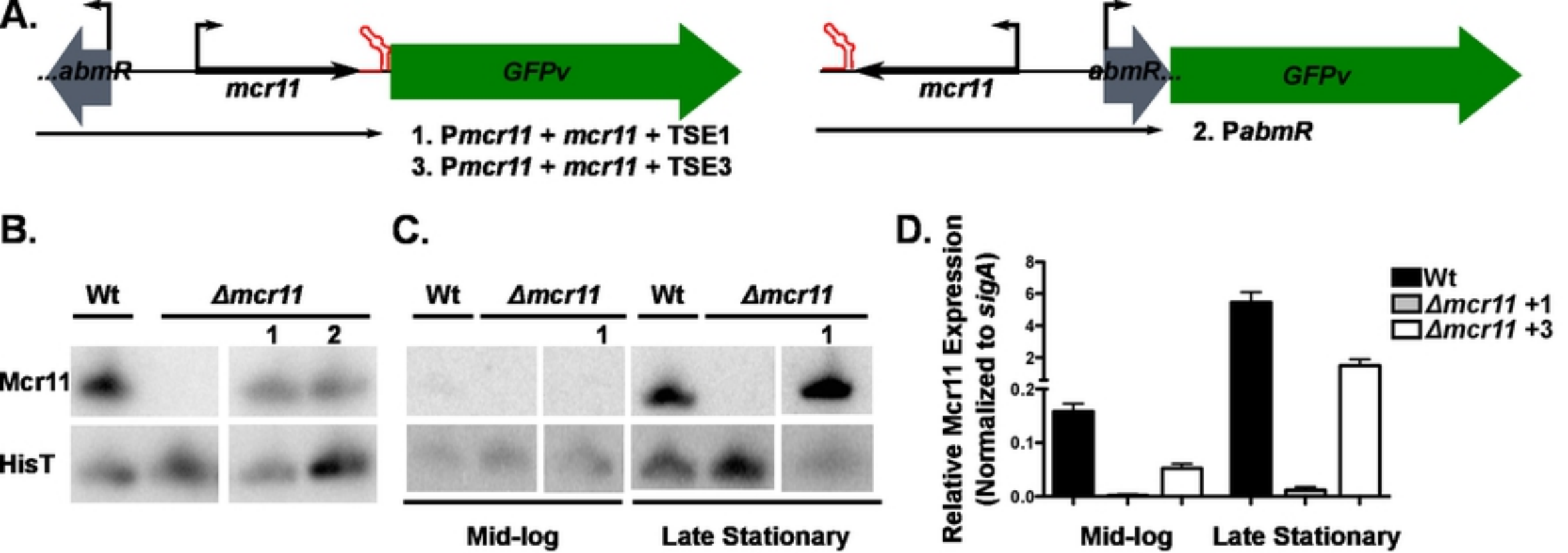
A.
...abmR
mcr11
GFPv
1. Pmcr11 + mcr11 + TSE1
3. Pmcr11 + mcr11 + TSE3
mcr11
abmR...
GFPv
2. PabmR
B.
Wt
Δmcr11
1
2
Mcr11
HisT
C.
Wt
Δmcr11
Wt
Δmcr11
1
1
Mid-log
Late Stationary
D.
Relative Mcr11 Expression
(Normalized to sigA)
8
6
4
2
0.2
0.1
0.0
Wt
Δmcr11 +1
Δmcr11 +3
Mid-log
Late Stationary

Figure 5

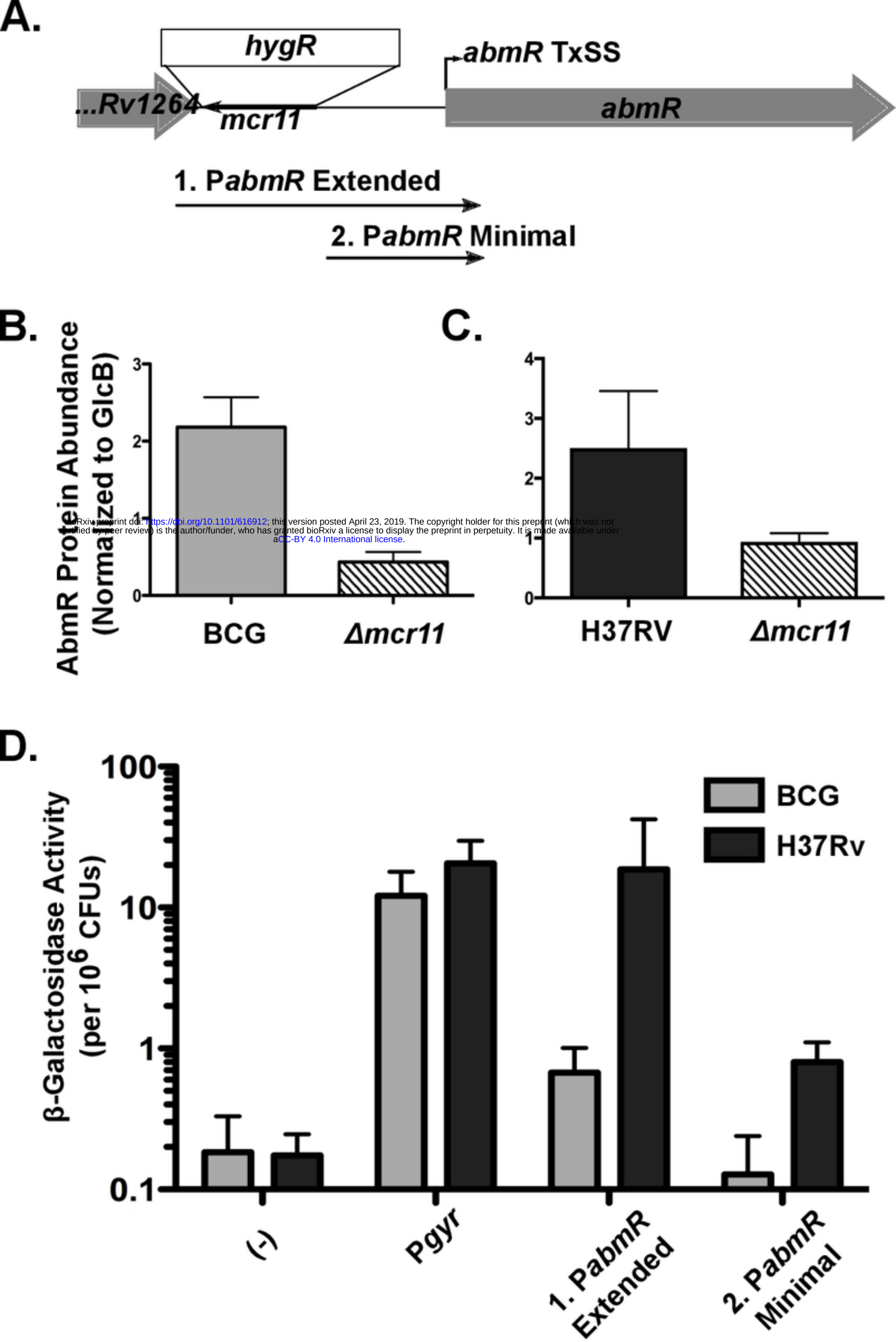

Figure 6

A.

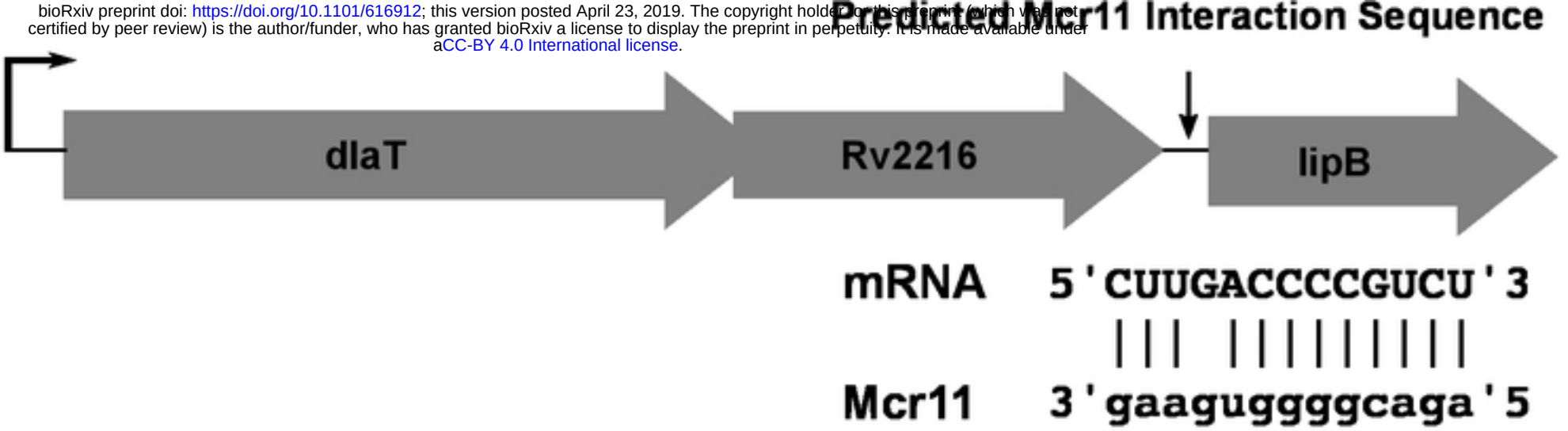

B.

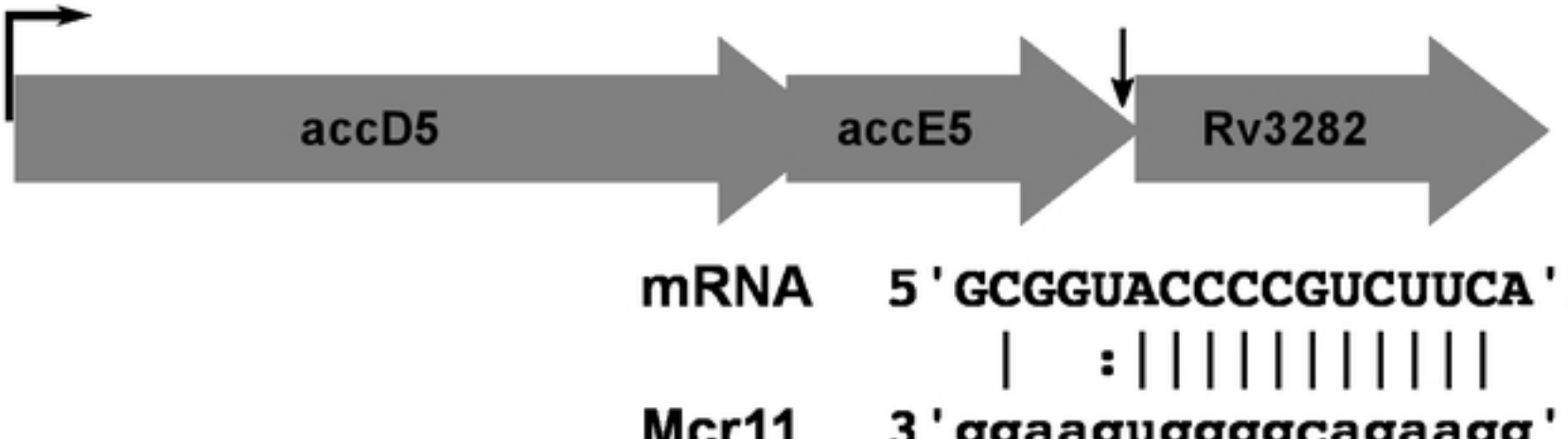

C. 5'**A**TC**G**AAGCAGGCCCGGTTAGTGACCAATCGAAAGTGCCGGAAGA
CGGGGTGAAGGCCGGCCGCGCAAGACCCGCAGAAGGCGGTGTCAGA
CGCCCCCCGAGAGTCACGCCGGGTCTGCC**CA** 3'

D.

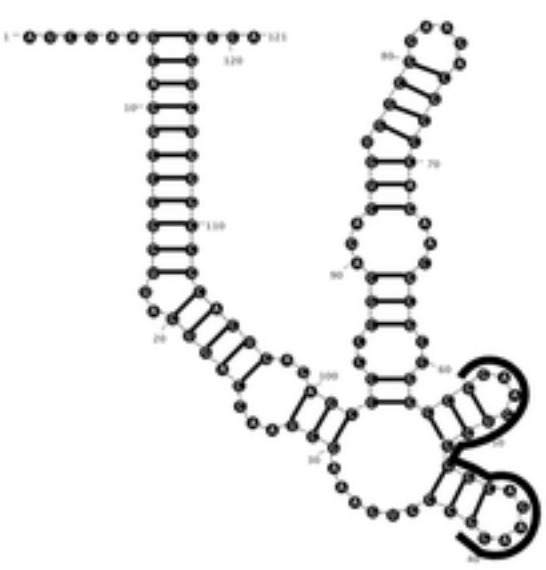

Figure 7

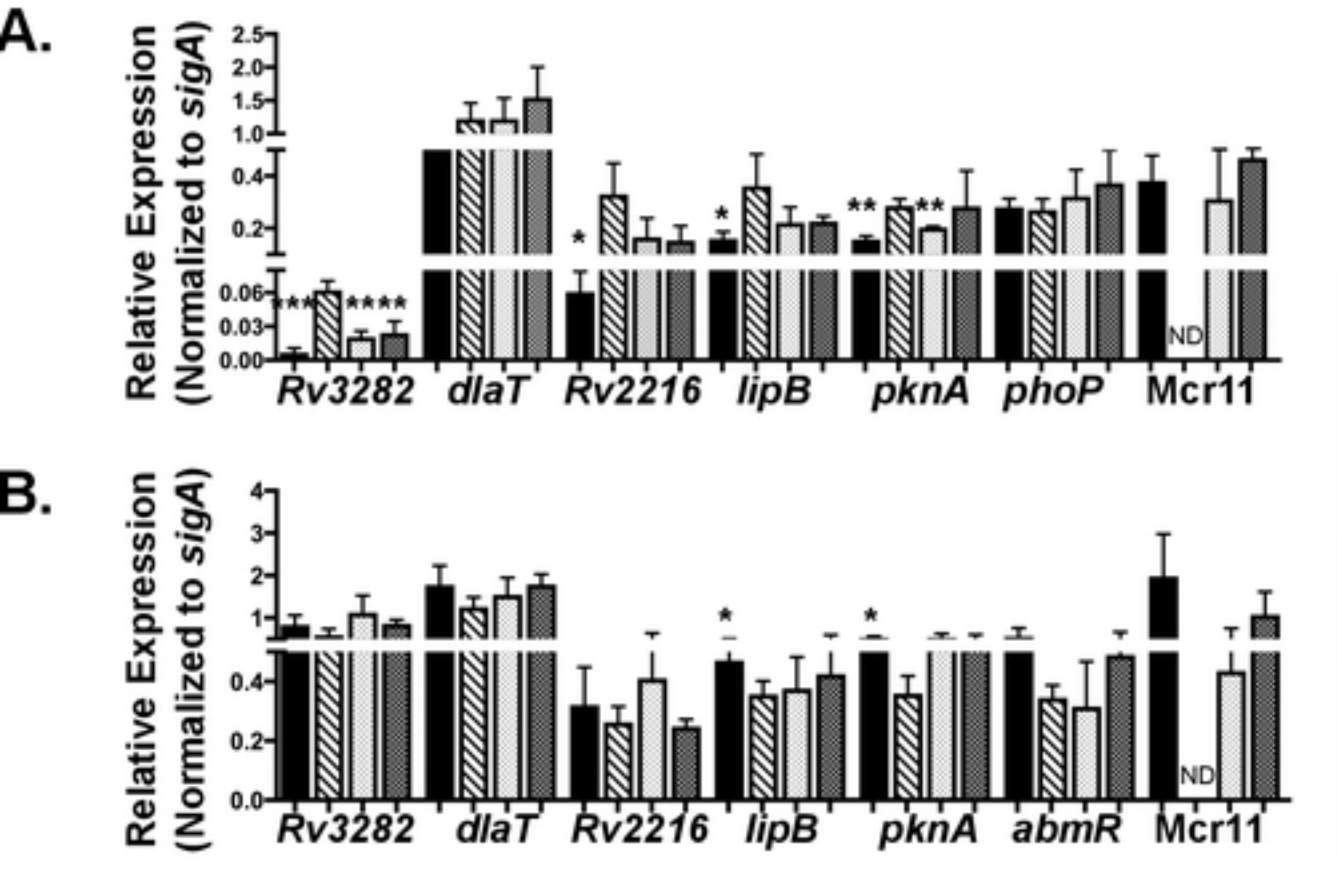

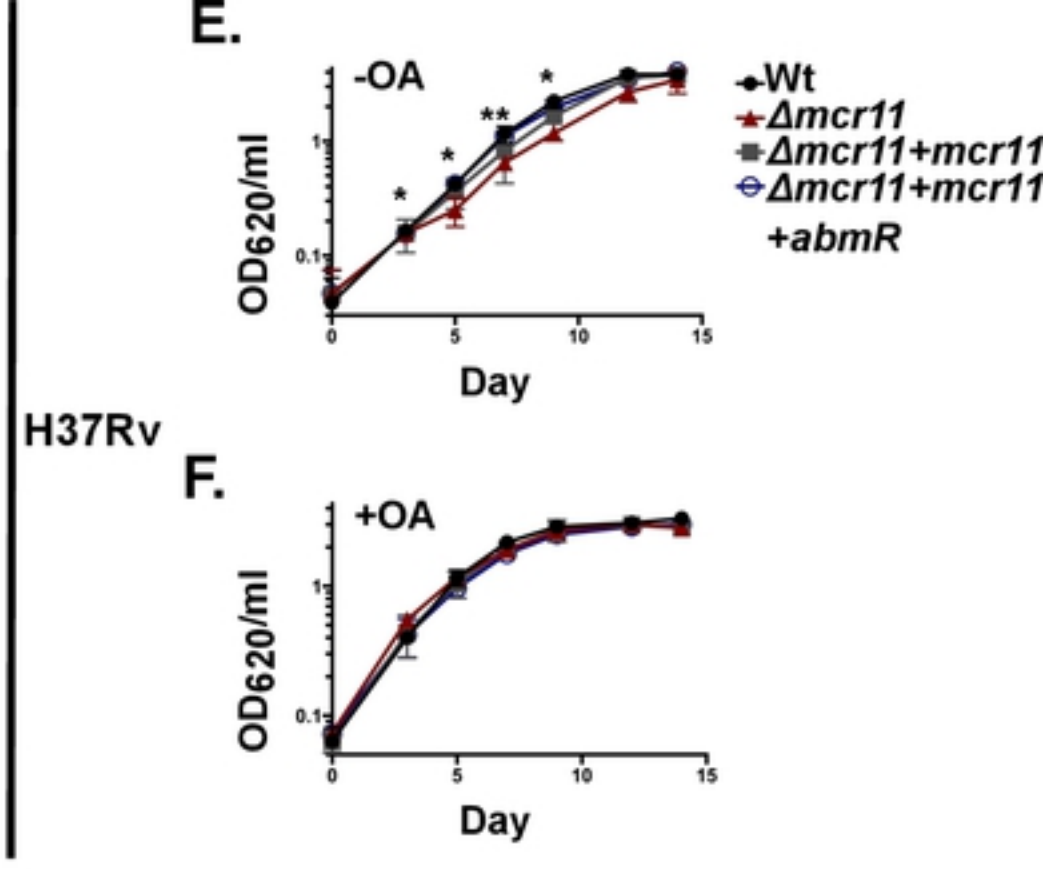

Figure 8

Figure 8

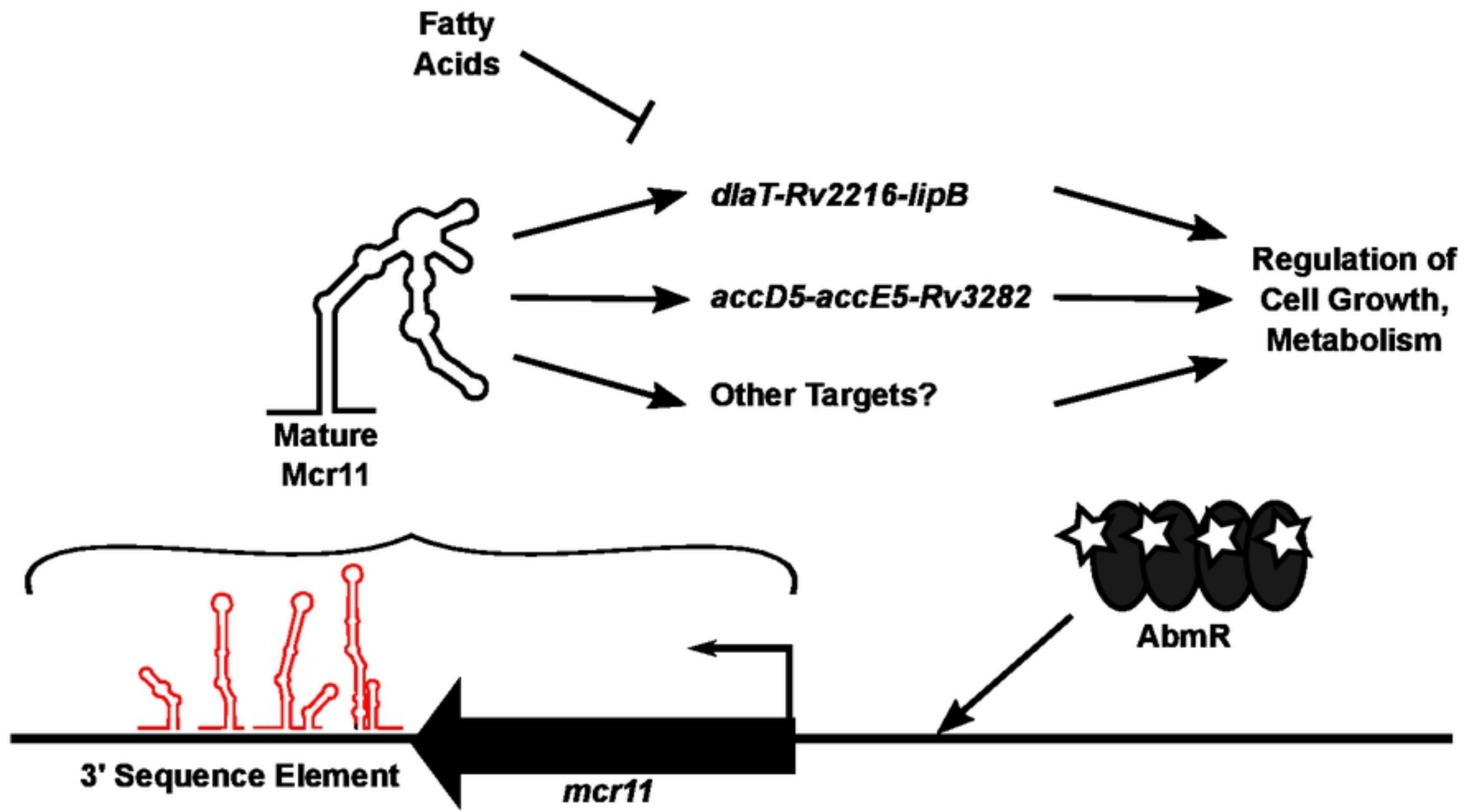
Fatty
Acids
dlaT-Rv2216-lipB
accD5-accE5-Rv3282
Other Targets?
Regulation of
Cell Growth,
Metabolism
Mature
Mcr11
AbmR
3' Sequence Element
mcr11

Figure 9

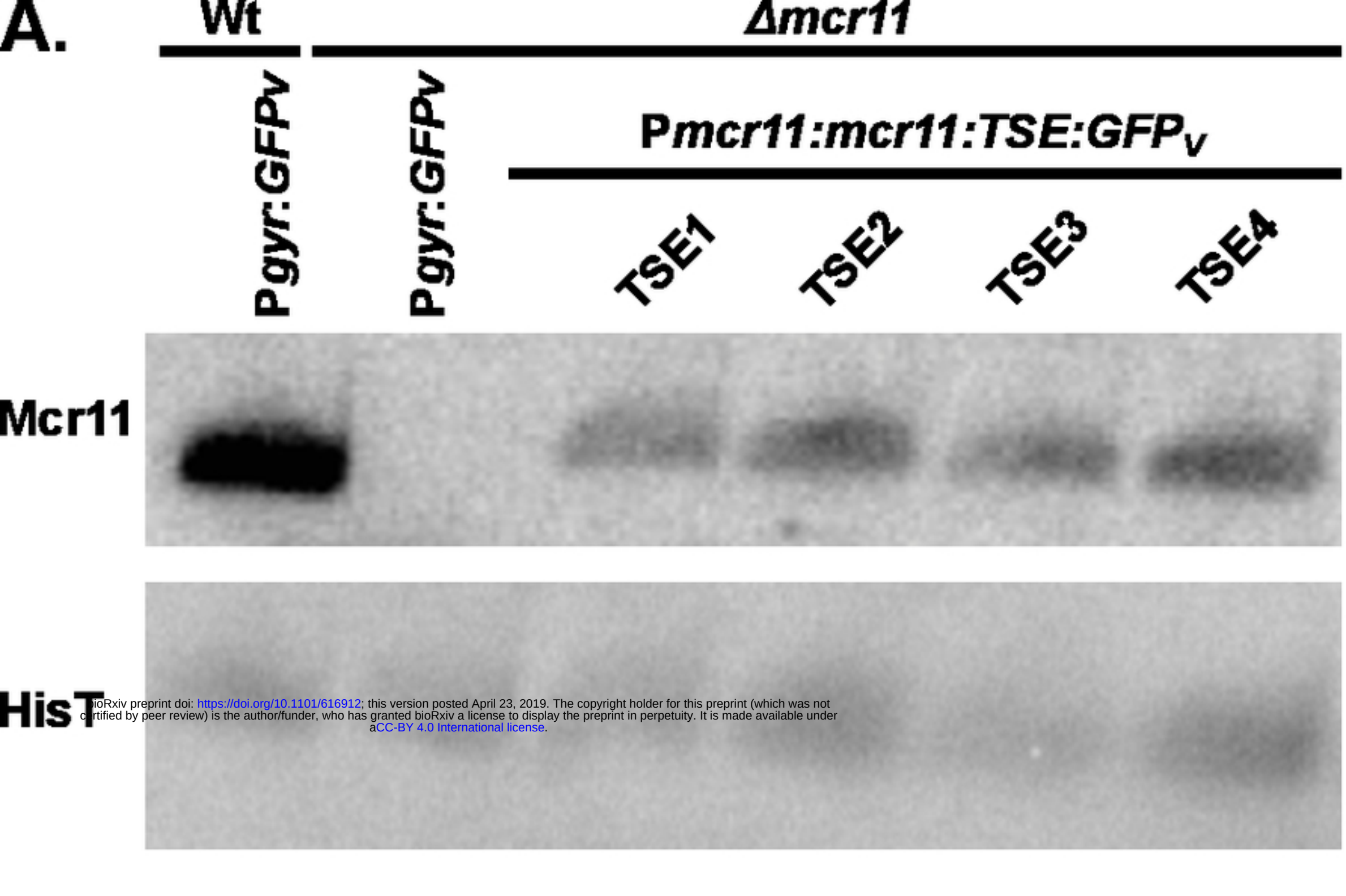

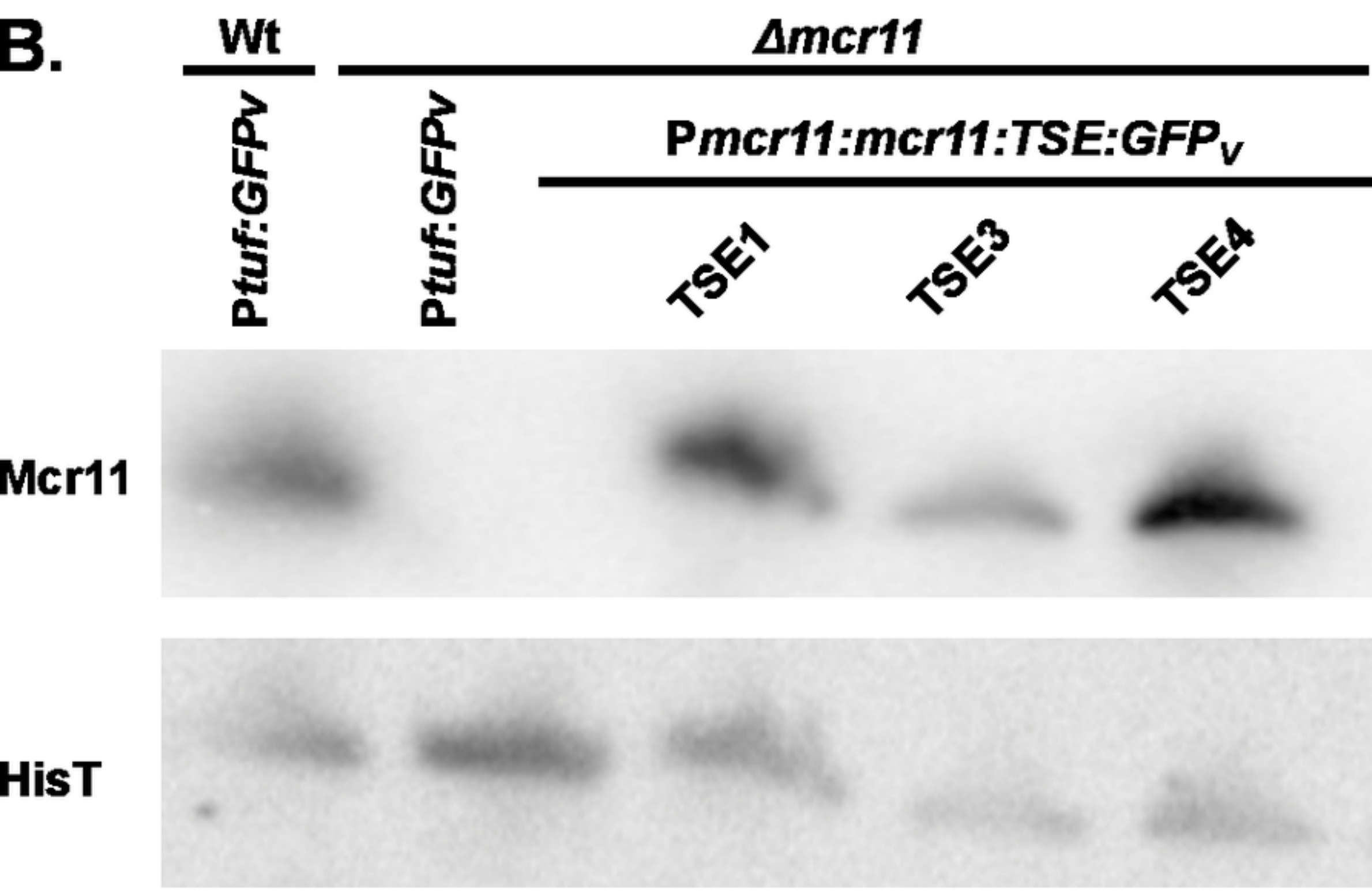

Figure 4